PK/PD modelling of glucose-insulin-glucagon dynamics in healthy dogs after a subcutaneous bolus administration of native glucagon or a novel glucagon analogue

Wendt, Sabrina Lyngbye; Møller, Jan Kloppenborg; Boye Knudsen, Carsten; Madsen, Henrik; Haidar, Ahmad ; Jørgensen, John Bagterp

Publication date:
2016

Document Version
Publisher's PDF, also known as Version of record

PK/PD modelling of glucose-insulin-glucagon dynamics in healthy dogs after a subcutaneous bolus administration of native glucagon or a novel glucagon analogue

Sabrina Lyngbye Wendt*[1,2,3], Jan Kloppenborg Møller[2], Carsten Boye Knudsen[1], Henrik Madsen[2], Ahmad Haidar[3,4], and John Bagterp Jørgensen[2]

[1]Department of Bioanalysis and Pharmacokinetics, Zealand Pharma A/S, Glostrup, Denmark
[2]Department of applied mathematics and computer science, Technical University of Denmark, Kongens Lyngby, Denmark
[3]Institut de Recherces Cliniques de Montréal, Montreal, Quebec, Canada
[4]Division of Experimental Medicine, McGill University, Montreal, Quebec, Canada

Version 1
April, 2016

DTU Compute Technical Report-2016-2. ISSN: 1601-2321.
* Email: slw@zealandpharma.com or slwe@dtu.dk

Objective We aim to develop a simulation model of the complex glucose-insulin-glucagon dynamics based on physiology and data. Furthermore, we compare pharmacokinetic (PK) and pharmacodynamic (PD) characteristics of marketed reconstituted glucagon with a stable liquid glucagon analogue invented by Zealand Pharma A/S.
Research Design and Methods We expanded a physiological model of endogenous glucose production with multiplicative effects of insulin and glucagon and combined it with the Hovorka glucoregulatory model. We used a Bayesian framework to perform multidimensional MAP estimation of model parameters given priors reported in the literature. We used profile likelihood analysis to investigate parameter identifiability and reduce the number of model variables. We estimated model parameters in pre-clinical data from one cross-over study with a total of 20 experiments in five dogs. The dogs received two subcutaneous (SC) bolus injections of low and high doses of glucagon and ZP-GA-1 (20 and 120 nmol/kg).
Results We report posterior probability distributions and correlations for all identifiable model parameters. Based on visual inspection and residual analysis, the PD model described data satisfactorily for both glucagon and the analogue. Parameter estimates of the PD model were not significantly different between the two compounds.
Conclusions The new PK/PD model enables simulations of the glucose-insulin-glucagon dynamics after a SC bolus of glucagon or glucagon analogue. The novel glucagon analogue by Zealand Pharma A/S shows PK and PD characteristics similar to marketed glucagon.

Keywords: Pharmacokinetics, PK, Pharmacodynamics, PD, modeling, modelling, glucagon, glucagon analogue, glucose, insulin, glucoregulatory, ODE, SDE, MAP, simulation, profile likelihood

Contents

1 Introduction **4**

2 Data **8**
2.1 Data collection . . . 8
2.1.1 Study 1 . . . 8
2.2 Bioavailability . . . 8
2.3 Unit conversion . . . 8
2.3.1 Glucagon . . . 9
2.3.2 Insulin . . . 9
2.4 Basal concentrations . . . 10
2.5 Data cleaning . . . 10

3 Models **11**
3.1 PK model . . . 11
3.2 PD model . . . 12
3.2.1 Version 1.0 - Integrating Emami in Hovorka . . . 12
3.2.2 Version 1.1 - Saturation of EGP . . . 14
3.2.3 Version 1.2 - Basal insulin . . . 14
3.2.4 Version 2.0 - Sigmoid E_{max} model . . . 15
3.2.5 Final PD model . . . 17

4 Methods **19**
4.1 Mathematical concepts . . . 19
4.1.1 Maximum likelihood . . . 19
4.1.2 Profile likelihood . . . 19
4.1.3 Bayesian inference . . . 20
4.1.4 Maximum a posteriori estimation . . . 20
4.1.5 Stochastic differential equations . . . 21
4.2 Application in CTSM-R . . . 21
4.2.1 Model structure . . . 21
4.2.2 Initial values . . . 22
4.2.3 Prior information . . . 22
4.2.4 Parameter identifiability . . . 25
4.2.5 Model fitting and validation . . . 26

5 Results **26**
5.1 PK . . . 27
5.1.1 Parameter estimates . . . 27
5.1.2 PK Model fits . . . 27
5.2 PD . . . 27
5.2.1 Reducing variables . . . 27
5.2.2 Model validity . . . 30
5.2.3 Residual Analysis . . . 30
5.2.4 PD Model fits . . . 31
5.2.5 Parameter estimates . . . 33
5.2.6 Native glucagon versus glucagon analogue . . . 35

6 Discussion **35**

References **39**

Appendix **43**

A Raw data **43**

B PK Model fits **46**

C PD model fits **49**

1 Introduction

Conventionally, diabetes type 1 is treated with multiple daily injections of insulin or continuous infusion of insulin using a pump. The stress of calculating the needed amount of insulin based on food intake, exercise and insulin sensitivity has led to research in creating an artificial pancreas (AP). A basic AP is a closed-loop (CL) system consisting of an insulin pump, a continuous glucose monitor (CGM) and a control algorithm to adjust insulin dosage through the pump based on CGM sensor readings.
Until recently, researchers and developers of the AP have mainly focused on a single hormone approach [1]. However, research in the field of dual hormone AP systems is growing substantially and clinical studies are being conducted by research groups in Boston [2–4], Montreal [5–8], Portland [9, 10], and Amsterdam [11–14]. In multiple studies of single hormone open-loop (OL) versus single hormone CL and/or dual hormone CL systems these groups have demonstrated that time in range increases when using a CL system compared to an OL system. Moreover, comparative studies show significant reduction of time spent in hypoglycaemia and number of hypoglycaemic events using a dual hormone CL system versus a single hormone CL system [6, 7, 9].

The unstable nature of native glucagon in liquid formulation challenges the development of a dual hormone AP. The hormone is currently marketed in dry form and needs reconstitution daily [16, 17]. Immediately after reconstitution glucagon starts degrading and forming fibrils. The fibrillation can cause the pump tubing to occlude and the degradation reduces the efficacy of the compound. Currently, only reconstituted glucagon is available for dual hormone AP studies which frequently experience glucagon pump occlusions [3, 13, 14].
At least two pharmaceutical companies are developing glucagon stable in liquid solution suitable for pump use. Xeris Pharmaceuticals Inc. is developing native glucagon stabilized in dimethyl sulfoxide (DMSO) [18], whereas Zealand Pharma A/S is developing a glucagon analogue in aqueous solution [19]. With this ongoing development of liquid stable glucagon suitable for pump use, the realization of a dual hormone AP is becoming practically possible.

In silico experiments are useful during the development of a control algorithm for a dual hormone AP

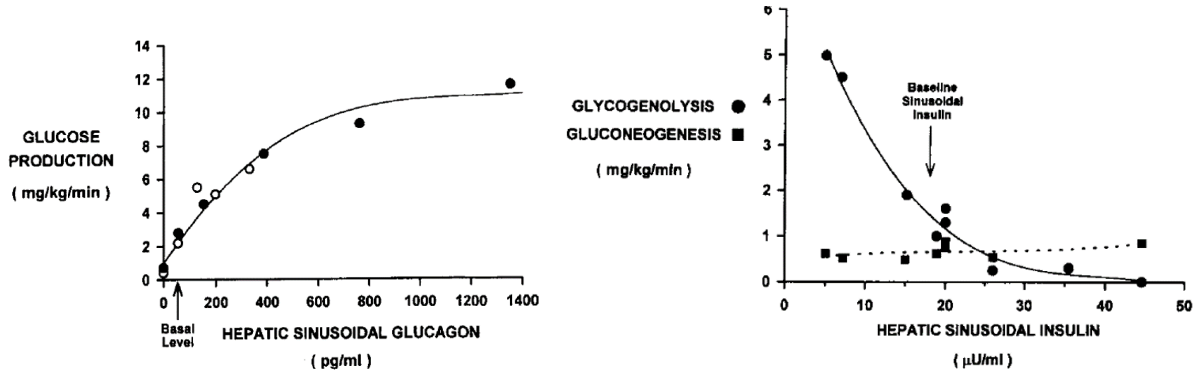

Figure 1: Endogenous glucose production due to glucagon and insulin. Left) The relationship between liver glucagon concentration and glucose production. Solid circles represent data from dogs, and open circles represent data from humans. Right) The relationship between liver insulin concentration and glucose production in dogs by gluconeogenesis and glycogenolysis. Data were acquired during basal arterial and portal glucagon concentrations, basal arterial insulin concentrations and mostly during euglycemia. Both graphs are from Cherrington [15].

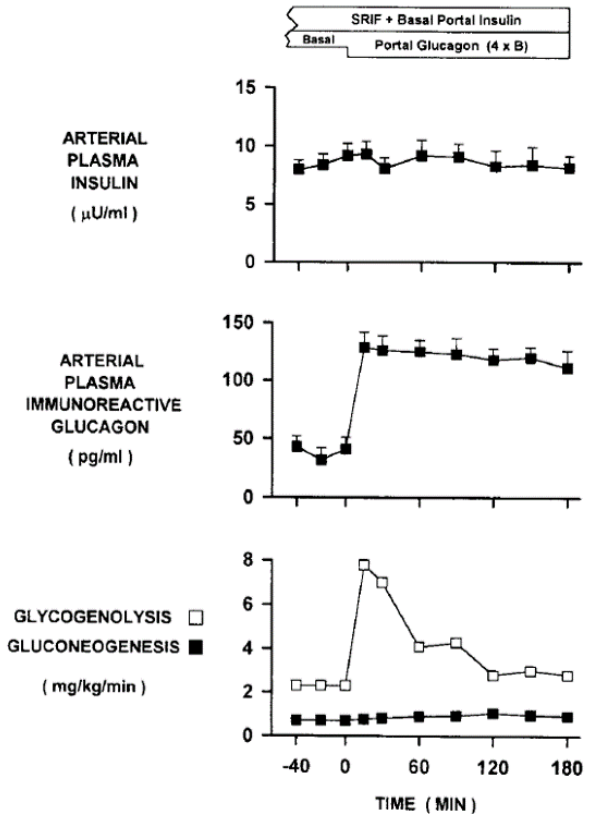

Figure 2: The effect of increased glucagon on glycogenolysis and gluconeogenesis in the dog. Somatostatin (SRIF) was given along with basal (B) replacement amounts of insulin and glucagon intraportally. At time zero the glucagon infusion rate was increased. The data is from Wada et al. [27].

before applying the algorithm in a clinical trial. Simulations *in silico* can also provide new insights in physiological system. A model describing the dynamics between glucose and insulin is validated by tracer data [20], and widely used in the literature for simulations of the endocrine regulatory system [21–23]. Recent proposed extensions include the effect of glucagon on endogenous glucose production (EGP) [24–26]. It is important to understand the glucose dynamics of the body to evaluate if these glucagon-glucose models are capturing the complexity of the reality.

The quantitative dynamics of insulin and glucagon on EGP are complex and not completely understood [15]. Two processes contribute to EGP: gluconeogenesis (GN) and glycogenolysis (GG). GN is the formation of glucose from non-carbohydrate substrates like glucogenic amino acids, glycerol, pyruvate and lactate. GG is the breakdown of stored glycogen in the liver to glucose. Studies show that glucagon and insulin have very little effect on GN as opposed to GG [15, 29, 30], see Figures 1 and 2. Thus the hormones influence mainly the EGP by regulating GG; glucagon stimulates it whereas insulin inhibits it. Increasing the glucagon concentration stimulates GG until a certain point where-after the response saturates. Saturation of response is typical for receptor mediated processes due to the limited number of receptors in a physiological system [31]. As opposed to glucagon, insulin inhibits GG and completely suppresses the breakdown of glycogen at insulin concentrations exceeding approximately 45 mIU/L [15]. A recent study by El Youssef et al. showed that at high insulin concentrations (46.0$\pm$12.5 mIU/L) the EGP is greatly reduced independent of the glucagon dose [28], see Figure 3. Moreover, the rates of EGP

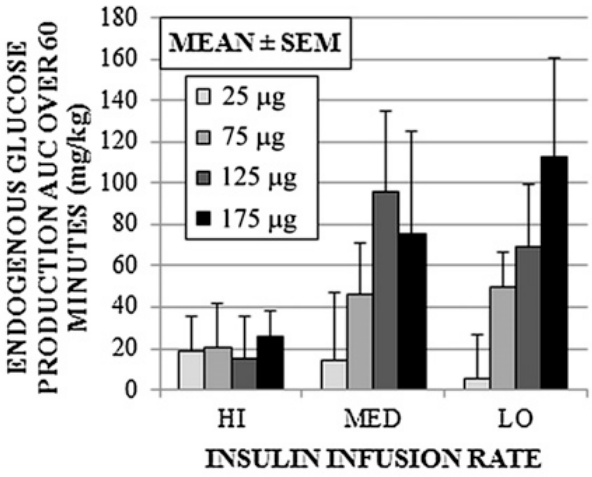

Figure 3: Endogenous glucose production with increasing glucagon doses (25, 75, 125, 175 μg) at high, medium and low insulin infusion rates (0.016±0.006 IU/kg/h, 0.032±0.003 IU/kg/h, 0.05±0.0 IU/kg/h) giving plasma insulin concentrations of 17.6±13.0 mIU/L, 29.1±8.9 mIU/L, and 46.0±12.5 mIU/L, respectively. The graph is from El Youssef et al. [28].

at high insulin concentrations match the rates of GN. The results are in agreement with previous studies showing that insulin suppresses GG but does not affect GN. These results suggest that the effect of insulin prevails over glucagon at high insulin concentrations. Some studies indicate that not only does the absolute glucagon concentration affect EGP but also the glucagon rate of change [15, 27].

The glucose kinetics model by Herrero et al. is based on the minimal model and describes the glucose changes with additive effects of insulin and of glucagon [25, 32]. The EGP model by Dalla Man et al. also describes the effects of insulin and of glucagon additively [24]. The glucose kinetics model of Hovorka includes the interaction of insulin and EGP, but does not describe the effect of glucagon on EGP [20]. The only model including the interaction and effect of both glucagon and insulin on EGP is proposed by Emami et al. [26]. This model approximates the EGP response to either glucagon or insulin with linear effects and includes the effect of glucagon rate of change on the EGP. The linear assumption of the EGP response to glucagon is fair as long as the glucagon concentration does not exceed approximately 400 pg/mL. Based on deviance information criterion the novel model outperformed several other models including the one proposed by Herrero et al. The model by Emami et al. assumes that the glycogen stores are never depleted. This is a valid assumption at normal conditions since a recent study showed that small repeated glucagon doses over a short time span did not significantly alter the glycogen stores even after an overnight fast [22].

This technical report presents a novel model of the glucose-insulin-glucagon dynamics by combining the validated insulin-glucose model and the physiological EGP model for the purpose of simulation. The insulin-glucose model by Hovorka et al. forms the basis of the dynamical system [20]. The model by Emami et al. extends the EGP part of the Hovorka model to include glucagon [26]. The EGP model is modified further to ensure saturation of the EGP at high glucagon concentrations in accordance with literature and physiological receptor activation concepts.

Furthermore, this report aims to thoroughly illustrate and explain the mathematical methods applied during the model fitting procedure of the pharmacodynamics model. The final model is fitted to individual

datasets using a multidimensional Bayesian framework. Parameter identifiability is investigated using profile likelihood analysis. Model validity is confirmed by estimating the noise contribution of the system using the grey-box modelling approach with stochastic differential equations (SDEs) [33]. After validation, final parameter estimation is conducted using the white-box modelling approach with ordinary differential equations (ODEs) making the model suitable for simulations. We use a programming environment in R created for continuous time stochastic modelling (CTSM) for the entire model fitting procedure [34].

Previously, PK data of this report were used for model fitting by a different technique and presented as a poster at the 8th International Conference on Advanced Technologies & Treatments for Diabetes (ATTD) in February 2015 [19]. PD results of this report were presented as a poster at the 9th ATTD in February 2016 [35].

Table 1: Data summary.

Study	Drug	Dose, nmol/kg	Dogs	Nominal Sample Times, minutes post dose
1	Glucagon	20	5	0, 5, 10, 15, 20, 30, 40, 50, 60, 75, 110, 140, 180
		120		
	ZP-GA-1	20		
		120		

2 Data

Zealand Pharma A/S is developing a new glucagon analogue with increased stability in liquid solution for treatment and better control of hypoglycemia in diabetes patients. The novel compound, ZP-GA-1, was tested against marketed glucagon (GlucaGen®, Novo Nordisk A/S) in pre-clinic. Both compounds are peptides and act as glucagon receptor agonists.

2.1 Data collection

Data originates from a pre-clinical study in dogs designed by Zealand Pharma A/S and conducted at Covance Laboratories Ltd (Covance site, Harrogate UK). The Institutional Animal Care and Use Committee approved the study and all procedures carried out on the dogs were in accordance with the Animals (Scientific Procedures) Act 1986. The study is summarized in Table 1 and described in Section 2.1.1.
Data was originally collected for the purpose of showing a PD effect of the glucagon analogue *in vivo* and to compare it with the PD effect of marketed glucagon.

2.1.1 Study 1

Five healthy Beagle dogs (bodyweight 13.6 $\pm$ 1.3 kg; mean $\pm$ SD) were included in this randomized cross-over study and named dog 1-5. At four dosing occasions each dog received a subcutaneous (SC) bolus injection of 20 or 120 nmol/kg glucagon or ZP-GA-1. Blood samples were collected at 0, 5, 10, 15, 20, 30, 40, 50, 60, 75, 110, 140, and 180 minutes after dose administration. Sample concentrations of glucagon and of ZP-GA-1 were analyzed using an in-house developed LC-MS/MS method. Plasma concentration of insulin was analyzed using a commercially available immunoassay from Meso Scale Discovery (MSD) (catalog no. K152BZC). Although the MSD assay was designed for mouse/rat plasma, an in-house validation showed that it was also valid for analysis of insulin in dog plasma. Plasma concentration of glucose was analyzed using Roche glucose method (UV test) [36]. Figure 4 presents an example of raw data from one dog in study 1.

2.2 Bioavailability

The bioavailability is obtained from the ratio between the dose-normalized area under the curve (AUC) after SC administration compared to IV. The AUC's were calculated using non-compartmental analysis (reported at Zealand Pharma A/S). The bioavailability varies between the drugs. Thus, for each drug the bioavailability is used in the input to the PK model, see summary in Table 2.

2.3 Unit conversion

In the study, glucagon and analogue concentrations were measured in nmol/L, insulin concentration was measured in pg/mL and glucose concentration was measured in mmol/L. Model parameters concerning glucagon and of insulin are often reported so that concentrations thereof should be in pg/mL and mIU/L,

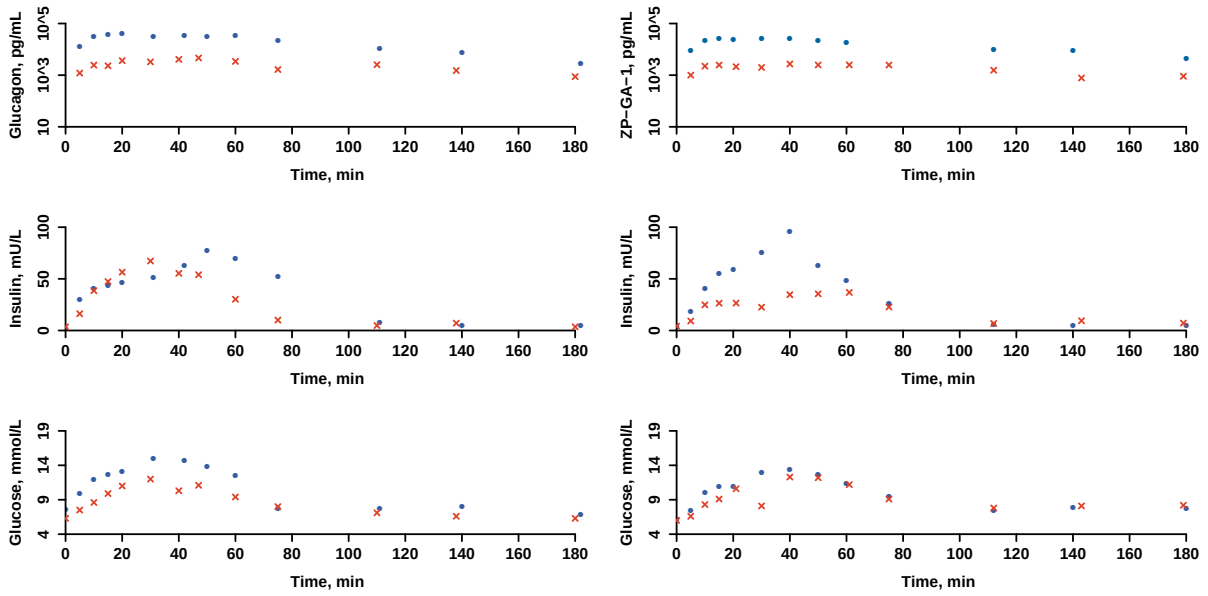

Figure 4: Raw data from dog 2 in study 1. Plasma concentrations after low or high doses of glucagon and ZP-GA-1 are red crosses or blue dots, respectively.

Table 2: Bioavailability and molar mass of glucagon and glucagon analogue in study 1.

Study	Drug	Bioavailability	Molar mass, g/mol
1	Glucagon	37.5%	3482.75
	ZP-GA-1	50%	3339.7

respectively [20,21,25]. The units of the PK and the PD data were converted to these generally used units before modelling.

2.3.1 Glucagon

To convert the plasma concentration of the administered compound from nmol/L to pg/mL, PK data is multiplied by the molar mass of the compound since the following yields units of pg/mL.

$$\frac{[\text{nmol}]}{[\text{L}]}\frac{[\text{L}]}{10^3\,[\text{mL}]}\frac{10^3\,[\text{pmol}]}{[\text{nmol}]}\frac{\text{MolarMass}\,[\text{pg}]}{[\text{pmol}]} \tag{1}$$

The molar masses of glucagon and the analogue are listed in table 2.

2.3.2 Insulin

To convert the insulin concentration from pg/mL to mIU/L, insulin PD data is multiplied by 0.023 since the following yields units of (mIU/L).

$$\frac{[\text{pg}]}{[\text{mL}]}\frac{10^3\,[\text{mL}]}{[\text{L}]}\frac{0.023\,[\text{IU}]}{[\mu\text{g}]}\frac{10^3\,[\text{mIU}]}{[\text{IU}]}\frac{[\mu\text{g}]}{10^6\,[\text{pg}]} \tag{2}$$

The assay used for analysis uses the WHO standard of 0.023 (IU/μg).

Table 3: List of removed outliers in the datasets substituted with linear interpolation of neighbouring observations. *Outlier not substituted by interpolation but removed.

Study	Dog	Drug	Dose, nmol/kg	Analyte	Time, min
1	1M	Glucagon	20	Glucagon	*6
1	1M	ZP-GA-1	20	Glucose	6
1	1M	ZP-GA-1	20	Glucose	16
1	2M	ZP-GA-1	20	Glucose	30
1	3M	Glucagon	20	Glucose	15
1	3M	Glucagon	20	Glucose	40

2.4 Basal concentrations

After an overnight fast in healthy human adults, the glucagon concentration is around 91 pg/mL (range 40-400 pg/mL) and the fasting insulin concentration is approximately 10-15 mIU/L [37]. Based on the two present studies, the basal insulin concentration in dogs are considerably lower with an average around 3 mIU/L and range 1.6-5.7 mIU/L, thus less than one third of the human basal insulin concentration. As there is a negative relationship between basal insulin concentration and insulin sensitivity in humans [38], this lower basal insulin concentration in dogs indicate a higher insulin sensitivity.
Basal glucagon concentration in dogs is around 41-54 pg/mL [27]. The lower level of quantification (LLOQ) for glucagon measured in study 1 was 0.2 nmol/L corresponding to nearly 700 pg/mL. All measurements at time zero were below LLOQ. The basal concentration of glucagon can thus not be determined in this study.

2.5 Data cleaning

No formal tests of the significance of an outlier were used but rather visual inspection. Table 3 lists all data points that the modeller considered to be outliers. The glucagon outlier appeared to have too high concentration after just 6 minutes, whereas the removed glucose observations showed sudden drops in glucose concentration that did not seem physiological. Figure 4 shows an example of such a data point with a drop at 30 minutes after the low dose of glucagon analogue ZP-GA-1. Figures 16-20 in Appendix A present raw data from all datasets including outliers.

3 Models

3.1 PK model

The glucagon pharmacokinetics (PK) are investigated using a simple model as formulated by Haidar et al. [39,40], defined in (3)-(5) and visualized in Figure 5. The PK model is a one-compartment model of the disturbance in plasma concentration from baseline after extravascular drug administration with first order absorption kinetics from the SC tissue to the plasma. The model has two states; the first corresponding to the SC tissue and the the second corresponding to the central compartment (plasma and instantaneous equilibrating tissues). The model includes two rate constants; one describing absorption from the SC tissue to the central compartment and another describing elimination from the central compartment. To minimize confusion, the parameter naming is kept as closely to the formulation by Haidar et al. as possible.

$$\frac{\mathrm{d}q_1(t)}{\mathrm{d}t} = u(t) - k_1 q_1(t) \qquad q_1(0) = 0 \tag{3}$$

$$\frac{\mathrm{d}q_2(t)}{\mathrm{d}t} = k_1 q_1(t) - k_2 q_2(t) \qquad q_2(0) = 0 \tag{4}$$

$$C(t) = \frac{k_2 q_2(t)}{\mathrm{w}Cl} \cdot 10^3 + C_b \tag{5}$$

Model input: $u(t) = \delta(t) \cdot \mathrm{Dose} \cdot \mathrm{bioavailability}$
Model observation: $C(t_n)$
Model output: $C(t)$
Fixed parameter(s): w, (C_b)
Model parameters: k_1, k_2, Cl, C_b

$C(t_n)$ is the measured glucagon concentration in plasma (nmol/L) at discrete timepoints, $n = 1, ..., N$. $C(t)$ is the simulated glucagon concentration in plasma at continuous time. C_b is the basal glucagon concentration in plasma (nmol/L). In case of administration of the glucagon analogue, C_b is fixed to zero as no basal level exists in the body.
w is the measured bodyweight (kg). Cl is the clearance rate normalized by weight (mL/kg/min). k_1 is the absorption rate constant and k_2 is the elimination rate constant (min^{-1}).
The concentration of glucagon in the central compartment is obtained by multiplying the content with an expression similar to per volume of distribution in (5). In classical PK it is trivial that clearance is equal to the product of the elimination rate constant and volume of distribution [31]. Since clearance is normalized by weight the denominator is multiplied by the bodyweight.
The bioavailability does not influence the fit of the model to data, but is necessary to get physiological parameter estimates of clearance. The Dose (nmol) is multiplied by the Dirac delta function to model the bolus injection at time zero.

A surrogate marker for the onset of action, t_{max}, is obtained analytically from the absorption and elimination rate constants.

$$t_{max} = \frac{\log(k_1/k_2)}{k_1 - k_2} \tag{6}$$

In (6) log is the natural logarithm.

3.2 PD model

3.2.1 Version 1.0 - Integrating Emami in Hovorka

The pharmacodynamics (PD) of glucagon and insulin on glucose are described by combining two published models. The glucose-insulin part of the model was published by Hovorka et al. [20] and listed in equations (7)-(12). A few changes to this model include removal of glucose input, removal of the labelled glucose kinetics, and parameter substitution of insulin sensitivities instead of ratios between activation and deactivation rate constants. To minimize confusion, the parameter naming is kept as closely to the original publication as possible. The model is initially in steady state, but could be initialized in any state.

$$\frac{\mathrm{d}Q_1(t)}{\mathrm{d}t} = -F_{01} - S_T x_1(t) Q_1(t) + k_{12} Q_2(t) + GG(t) \quad Q_1(0) = Q_{10} \tag{7}$$

$$\frac{\mathrm{d}Q_2(t)}{\mathrm{d}t} = S_T x_1(t) Q_1(t) - \left[k_{12} + S_D x_2(t)\right] Q_2(t) \qquad Q_2(0) = Q_1(0) \frac{x_1(0)}{x_2(0) + k_{12}} \tag{8}$$

$$G(t) = \frac{Q_1(t)}{\mathrm{V}} \tag{9}$$

$$\frac{\mathrm{d}x_1(t)}{\mathrm{d}t} = k_{a1}[I(t) - x_1(t)] \qquad x_1(0) = \mathrm{I}_b \tag{10}$$

$$\frac{\mathrm{d}x_2(t)}{\mathrm{d}t} = k_{a2}[I(t) - x_2(t)] \qquad x_2(0) = \mathrm{I}_b \tag{11}$$

$$\frac{\mathrm{d}x_3(t)}{\mathrm{d}t} = k_{a3}[I(t) - x_3(t)] \qquad x_3(0) = \mathrm{I}_b \tag{12}$$

$$\tag{13}$$

The model is extended to include a GG model as proposed by Emami et al. [26], defined in equations (14)-(15). The combined PD model is visualized in figure 5.

$$\begin{aligned} GG(t) &= (1 - S_E x_3(t)) \cdot (S_{gd} E_{gd}(t) + S_g C(t)) \\ &\quad \text{where } 1 - S_E x_3(t) \geq 0 \text{ and } S_{gd} E_{gd}(t) + S_g C(t) \geq 0 \end{aligned} \tag{14}$$

$$\frac{\mathrm{d}E_{gd}(t)}{\mathrm{d}t} = -k_{gd} \left(E_{gd}(t) - \frac{\mathrm{d}C(t)}{\mathrm{d}t} \right) \tag{15}$$

Since CTSM-R does not accept if statements to supplement the state equations, the conditional statements are implemented as $\frac{1}{2} + \frac{1}{2} \cdot \tanh(100 \cdot "conditionalstatement")$ multiplied by the conditional statement. Thus, when the statement is positive the expression equals one, and when the statement is negative the expression is zero.
The PD model not only includes a term for the absolute concentration of glucagon, but also a term describing the glucagon rate of change in (15). The analytical solution to the glucagon rate of change is derived from (4)-(5) yielding units of nmol/L/min.

$$\frac{\mathrm{d}C(t)}{\mathrm{d}t} = \frac{k_2}{\mathrm{w}Cl} \cdot 10^3 \cdot (k_1 q_1(t) - k_2 q_2(t)) \tag{16}$$

Model inputs: $C(t)$, $\frac{\mathrm{d}C(t)}{\mathrm{d}t}$, $I(t)$
Model observation: $G(t_n)$
Model output: $G(t)$
Fixed parameters: V, I_b
Model parameters: F_{01}, k_{12}, S_T, S_D, S_E, k_{a1}, k_{a2}, k_{a3}, S_g, S_{gd}, k_{gd}

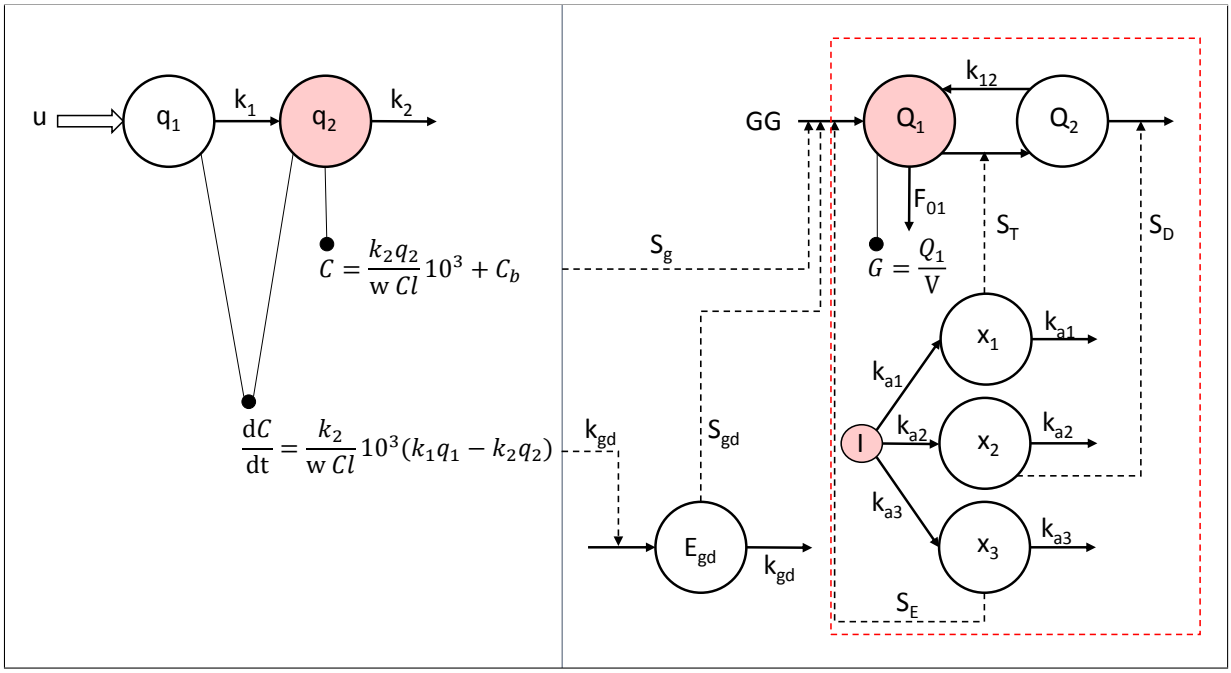

Figure 5: Schematic presentation of the full model including the PK part at the left and the PD part at the right. The open arrow symbolizes SC input of glucagon. Solid arrows indicate mass transfer to/from a compartment. Dashed arrows indicate effect without mass transfer. Solid lines ending with a dot indicate how an output is derived from the content of a compartment. Plasma compartments of glucagon, insulin and glucose are colored. A red dashed square surrounds the part of the model published by Hovorka et al. [20].

$C(t)$ and $\frac{\mathrm{d}C(t)}{\mathrm{d}t}$ are the simulated concentration (pg/mL) and rate of change (pg/mL/min) of glucagon in plasma at all times, respectively. $I(t_n)$ is the measured insulin concentration in plasma (mIU/L) at discrete timepoints, $n = 1, ..., N$. To match the time resolution of the glucagon input, the insulin observations are linearly interpolated to give the model input $I(t)$.
$G(t_n)$ is the measured glucose concentration in plasma (mmol/L) at discrete timepoints, $n = 1, ..., N$. $G(t)$ is the simulated glucose concentration in plasma at all times.
I_b is the basal insulin concentration for each dog averaged over a maximum of four occasions (mIU/L). V is the glucose volume of distribution and is fixed to 160 mL/kg based on literature [20].
F_{01} is the net total non-insulin-dependent glucose out-flux from the plasma compartment $\left(\frac{\mu\mathrm{mol}}{\mathrm{kg}\cdot\mathrm{min}}\right)$. GN is included in F_{01} and assumed constant and independent of insulin and glucagon as this process is affected very little by the two hormones. k_{12} is the transfer rate constant from the non-accessible glucose compartment to the accessible plasma compartment (min^{-1}). S_T is the insulin sensitivity on glucose transport (min^{-1} per mIU/L). S_D is the insulin sensitivity on glucose disposal (min^{-1} per mIU/L). S_E is the insulin sensitivity on EGP (1/(mIU/L)). k_{a1}, k_{a2} and k_{a3} are insulin deactivation rate constants (min^{-1}).
S_g is the glucagon sensitivity on GG $\left(\frac{\mu\mathrm{mol}}{\mathrm{kg}\cdot\mathrm{min}}\mathrm{per\ pg/mL}\right)$. E_{gd} is a fictive rate of change compartment contributing to rate of change of GG due to glucagon rate of change (pg/mL/min). S_{gd} is the glucagon rate of change sensitivity on GG $\left(\frac{\mu\mathrm{mol}}{\mathrm{kg}}\mathrm{per\ pg/mL}\right)$. k_{gd} is the delay of glucagon rate of change on EGP (min^{-1}).
The full PK-PD model is presented in figure 5.

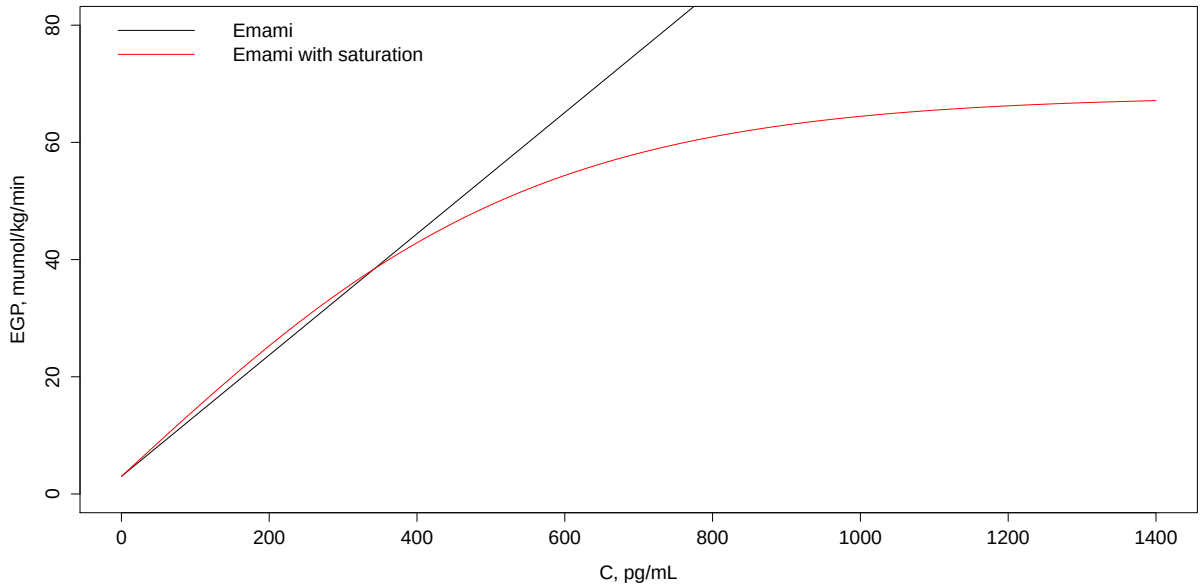

Figure 6: Comparison of GG model by Emami et al. [26] and modified model capturing the physiological saturation effect of glucagon on GG. The saturation part is proposed roughly to the data presented by Cherrington [15], compare with Figure 1. The graphed models assume basal insulin concentration and constant glucagon concentration. The curves do not start in (0,0) as GN is included.

3.2.2 Version 1.1 - Saturation of EGP

As reviewed in Section 1, GG saturates for some concentration of glucagon at basal insulin concentration, see Figure 1. The model stated in (14) is a linear approximation of the GG response to constant glucagon concentration and only covers the linear range of the dose response curve. No saturated data was available during the model development and therefore this dynamic was not captured in the model. However, the available data from Zealand Pharma A/S takes on very high concentrations of plasma glucagon and thus we assume that the GG response to glucagon is saturated for some parts of the studies if not the entire study duration. The GG model in (14) is modified to saturate GG at 65 $\frac{\mu\text{mol}}{\text{kg}\cdot\text{min}}$ at basal insulin level. The saturation is approximated by a simple tangent hyperbolic function and figure 6 confirms that the linear part of the curve resembles the original linear formulation at basal insulin concentration. The GG model with saturation is

$$\begin{aligned} GG(t) &= (1 - S_E x_3(t)) \cdot \frac{65}{0.69} \tanh\left(\frac{2.5}{1400} \cdot \frac{S_{gd}E_{gd}(t) + S_g C(t)}{S_g}\right) \\ &\text{where } (1 - S_E x_3(t)) \geq 0 \text{ and } (S_{gd}E_{gd}(t) + S_g C(t)) \geq 0 \end{aligned} \tag{17}$$

3.2.3 Version 1.2 - Basal insulin

Dogs have lower basal insulin concentrations than humans ($\sim$3 mIU/L versus $\sim$10 mIU/L), as described in section 2.4. Therefore, we can not assume that $(1 - S_E x_3(t))$ equals 0.69 at basal as in humans (calculated as $\text{EGP}_b/\text{EGP}_0$ from Hovorka et al. [20]). The model is thus changed to

$$\begin{aligned} GG(t) &= \frac{(1 - S_E x_3(t))}{(1 - S_E \text{I}_b)} \cdot 65 \cdot \tanh\left(\frac{2.5}{1400} \cdot \frac{S_{gd}E_{gd}(t) + S_g C(t)}{S_g}\right) \\ &\text{where } (1 - S_E x_3(t)) \geq 0 \text{ and } (S_{gd}E_{gd}(t) + S_g C(t)) \geq 0 \end{aligned} \tag{18}$$

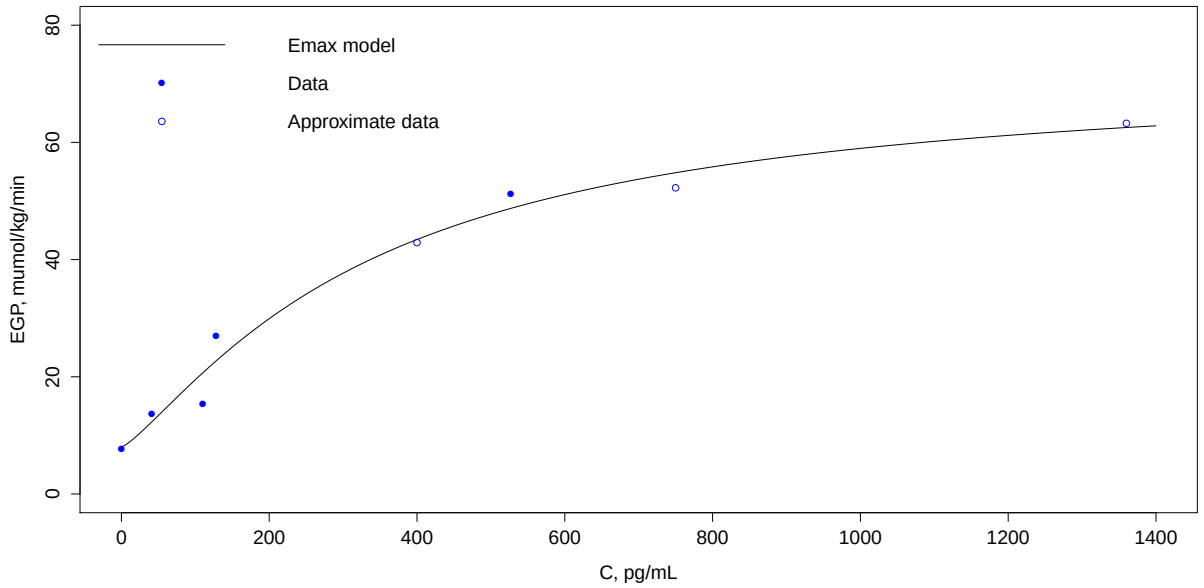

Figure 7: Relationship between plasma glucagon concentration and EGP. GN is constant and the GG is fitted with a sigmoid E_{max} model. The graph assumes basal insulin concentration. The solid data points originate from [27,41,42] and the open dots are approximated from [15] since the original data could not be retrieved. Note that EGP is not zero at zero glucagon due to the glucagon independent GN.

The change ensures that GG saturates at 65 $\frac{\mu\text{mol}}{\text{kg}\cdot\text{min}}$ at basal insulin concentration. Moreover, this addition ensures that at higher insulin levels than basal, the saturation value of GG is lower than 65 $\frac{\mu\text{mol}}{\text{kg}\cdot\text{min}}$. Similarly, at lower insulin levels than basal the saturation value of GG is higher than 65 $\frac{\mu\text{mol}}{\text{kg}\cdot\text{min}}$. Qualitatively speaking, insulin "modulates" the maximum GG response to glucagon.

3.2.4 Version 2.0 - Sigmoid E_{max} model

As discussed by Emami et al., the glucagon rate of change was added to the model to be able to capture the weakened response to a constant plasma glucagon concentration [26], also see Figure 2. Since we do not have data to describe this phenomenon and do not have a physiological explanation for how rate of change affects the GG response, we simplify the GG model to only depend on the absolute concentration of glucagon. We justify this with reference to Emami et al. who found that the GG model using both absolute glucagon concentration and glucagon rate of change was only slightly better than a similar model using only the absolute glucagon concentration [26].
To make the model parameters more physiological interpretable, we substitute the empirical tangent hyperbolic saturation model with the sigmoid E_{max} model which is used to describe receptor mediated kinetics [43]. The sigmoid E_{max} model is essentially a first order process at low concentrations, and a zero order process at high concentrations [31]. The model by Emami et al. in (14) describes the first order process and is approximated from data where first order kinetics apply [26]. The effect of plasma glucagon on the GG response is reformulated to comply with literature data [15,27,41,42], and the mean prior parameter values of this model are identified by optimization. The data used to fit the parameters and the optimal solution is presented in Figure 7. The new GG model and the fitted parameters are listed

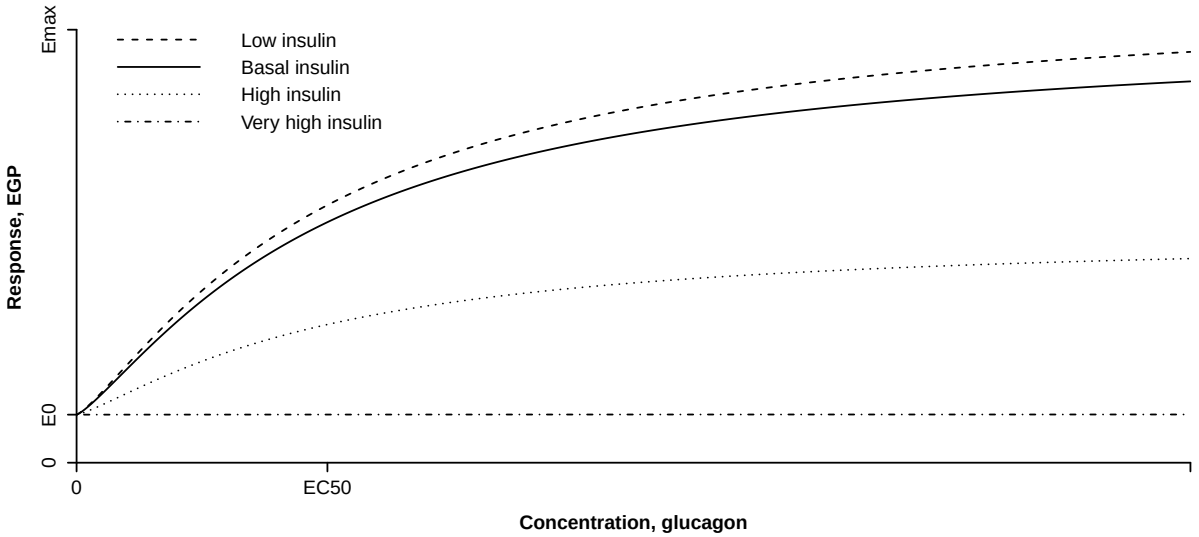

Figure 8: Qualitative visualization of the consequences of the multiplicative GG model showing how the total EGP response to glucagon changes at low, basal, high and very high insulin concentrations.

in (19).

$$GG(t) = \frac{(1 - S_E x_3(t))}{(1 - S_E \mathrm{I}_b)} \cdot \left((E_{max} - E_0) \frac{C(t)^\gamma}{EC_{50}^\gamma + C(t)^\gamma} \right) \text{ where } (1 - S_E x_3(t)) \geq 0 \tag{19}$$

$$E_{max} = 72.1 \, \frac{\mu\text{mol}}{\text{kg} \cdot \text{min}}, \quad E_0 = 8 \, \frac{\mu\text{mol}}{\text{kg} \cdot \text{min}}, \quad EC_{50} = 337.8 \, \frac{\text{pg}}{\text{mL}}, \quad \gamma = 1.25$$

The model describing the saturation of EGP due to glucagon consists of four parameters - two describing the minimum and maximum effect, E_0 and E_{max}, and two describing the curvature, EC_{50} and γ. E_0 is describing GN. EC_{50} is the concentration at the half maximum effect. The parameter γ reflects the number of molecules binding to one receptor and determines the steepness of the curve. We hypothesize that E_0 and E_{max} will be identical whether using marketed glucagon or the analogue. However, the parameters describing the curvature, i.e. the potency, might differ. Figure 8 visualizes the GG model with the multiplicative effect of glucagon and insulin qualitatively.

3.2.5 Final PD model

The equations describing the glucose-insulin-glucagon PD model are listed in (20)-(26) and the model visualized in Figure 9.

$$\frac{\mathrm{d}Q_1(t)}{\mathrm{d}t} = -F_{01} - S_T x_1(t) Q_1(t) + k_{12} Q_2(t) + GG(t) \qquad Q_1(0) = Q_{10} \tag{20}$$

$$\frac{\mathrm{d}Q_2(t)}{\mathrm{d}t} = S_T x_1(t) Q_1(t) - \left[k_{12} + S_D x_2(t)\right] Q_2(t) \qquad Q_2(0) = Q_1(0) \frac{x_1(0)}{x_2(0) + k_{12}} \tag{21}$$

$$GG(t) = \frac{(1 - S_E x_3(t))}{(1 - S_E \mathrm{I}_b)} \cdot \left((E_{max} - E_0) \frac{C(t)^\gamma}{EC_{50}^\gamma + C(t)^\gamma} \right) \text{ where } (1 - S_E x_3(t)) \geq 0 \tag{22}$$

$$G(t) = \frac{Q_1(t)}{\mathrm{V}} \tag{23}$$

$$\frac{\mathrm{d}x_1(t)}{\mathrm{d}t} = k_{a1}[I(t) - x_1(t)] \qquad x_1(0) = \mathrm{I}_b \tag{24}$$

$$\frac{\mathrm{d}x_2(t)}{\mathrm{d}t} = k_{a2}[I(t) - x_2(t)] \qquad x_2(0) = \mathrm{I}_b \tag{25}$$

$$\frac{\mathrm{d}x_3(t)}{\mathrm{d}t} = k_{a3}[I(t) - x_3(t)] \qquad x_3(0) = \mathrm{I}_b \tag{26}$$

Model inputs: $C(t)$, $I(t)$
Model observation: $G(t_n)$
Model output: $G(t)$
Fixed parameters: V, I_b
Model parameters: F_{01}, k_{12}, S_T, S_D, S_E, k_{a1}, k_{a2}, k_{a3}, E_0, E_{max}, EC_{50}, γ

The parameters and their units are described in previous sections 3.2.1-3.2.4.
We assume that F_{01} is constant at all times since we are not measuring any glucose concentrations below 4.5 mmol/L in the datasets to be fitted. However, for simulation purposes it is important to include the extended formulation of F_{01} taking the current glucose concentration into account [23].

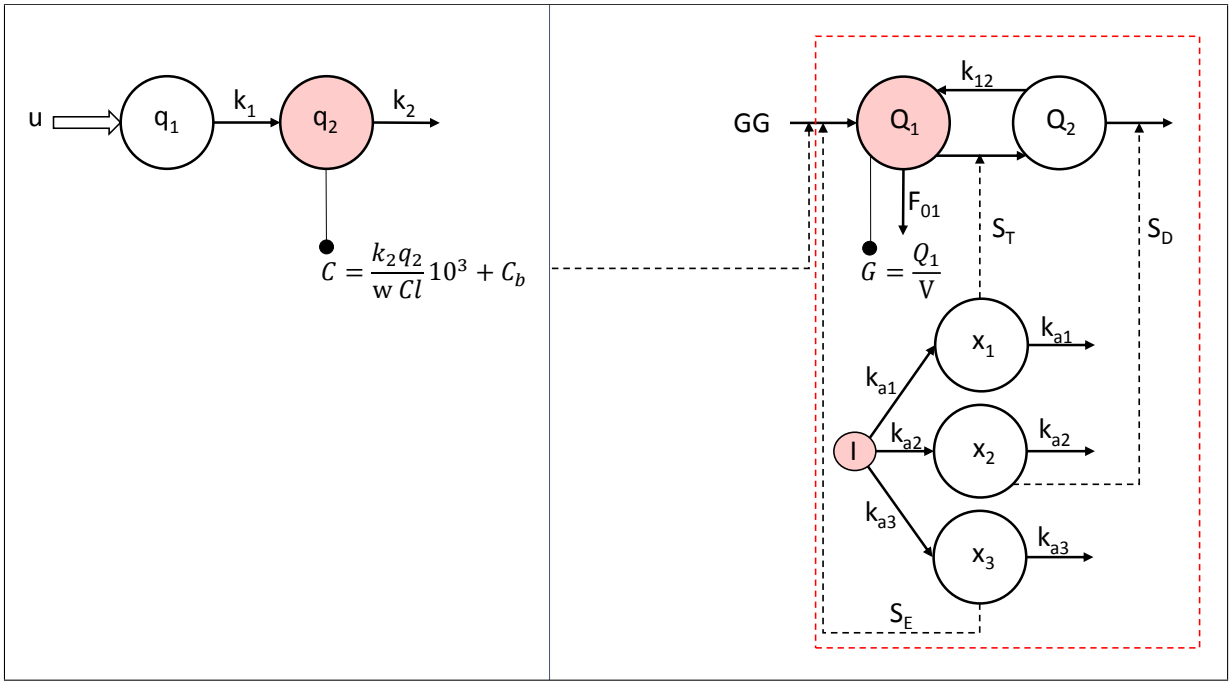

Figure 9: Schematic presentation of the final full model including the PK part at the left and the PD part at the right. The open arrow symbolizes SC input of glucagon. Solid arrows indicate mass transfer to/from a compartment. Dashed arrows indicate effect without mass transfer. Solid lines ending with a dot indicate how an output is derived from the content of a compartment. Plasma compartments of glucaogn, insulin, and glucose are colored. A red dashed square surrounds the part of the model published by Hovorka et al. [20].

4 Methods

4.1 Mathematical concepts

4.1.1 Maximum likelihood

The likelihood measures how likely a set of parameters are given data and a model. The likelihood is equal to the probability density considered as a function of the parameter set, θ, and a time series, Y_N, of N observations.

$$L(\theta, Y_N) = p(Y_N|\theta) \tag{27}$$

Different parameters of the model will give different values of the likelihood function. Finding the parameter set that maximizes the likelihood function for given data and a model gives the maximum likelihood (ML).

4.1.2 Profile likelihood

For a parameter, θ_i, and a time series, Y_N, of N observations, we can calculate the profile likelihood, which is defined as

$$L_p(\theta_i, Y_N) = \max_{\theta \setminus \theta_i} L(\theta, Y_N) \tag{28}$$

For a fixed value of θ_i the likelihood function is maximized across all other parameters of the parameter set θ which yields the profile likelihood of parameter θ_i [44, 45]. The profile likelihood of a parameter can be used to evaluate whether the parameter in the model is identifiable. Identifiability of parameters are determined by model structure (structural identifiability) and the input dynamics (practical identifiability) [44].
Structural identifiability is related to the transfer function from the input to the output. However, in large complex systems where the transfer function is non-trivial to derive, profile likelihood analysis provides a method for investigating the parameter identifiability.
Practical identifiability is related to the dynamics of the input. Thus, a model can only identify parameters describing dynamics present in data used for model fitting. Also in this case, profile likelihood analysis is a powerful tool.

A parameter is identifiable only if the maximum of the profile likelihood is well defined [44]. Whether the maximum of the profile likelihood of θ_i is well defined is evaluated using a 100(1-α)% confidence interval bound by when the natural logarithm of a likelihood ratio test exceeds a chi-squared distribution [45].

$$\log\left(\frac{L_p(\theta_i, Y_N)}{L(\hat{\theta}, Y_N)}\right) = \log(L_p(\theta_i, Y_N)) - \log(L(\hat{\theta}, Y_N)) > -\frac{1}{2}\chi^2_{1-\alpha} \tag{29}$$

In words, the profile likelihood is log-transformed yielding the profile log-likelihood. The maximum value of the profile log-likelihood is subtracted from the profile log-likelihood so that the maximum function value is zero. The limit of the confidence interval is determined by the 100(1-α) percentile of the chi-squared distribution with one degree of freedom. As an example, a 95% confidence interval of a model parameter is bound by the log-likelihood ratio exceeding approximately -1.92. A profile likelihood confidence interval could be asymmetric, whereas e.g. the Wald statistic applies a quadratic and thus symmetric approximation of the confidence interval [45].

4.1.3 Bayesian inference

Bayesian estimates refer to parameters of a model being treated as random variables belonging to some distribution. To fit a parameter in a Bayesian framework a prior distribution of the parameter is needed. The parameters of the prior distribution are called hyper-parameters i.e. if a prior follows a normal distribution, two hyper-parameters define it: mean and standard deviation (SD). The estimated parameter will then be a summary of the posterior probability density function conditioned on the data.
The posterior distribution of a parameter, θ, given the data, Y_N, is identified using Bayes' theorem:

$$p(\theta, Y_N) = \frac{p(Y_N|\theta)p(\theta)}{p(Y_N)} \tag{30}$$

where $p(\theta)$ is the prior distribution of θ, $p(Y_N)$ is the marginal distribution and $p(Y_N|\theta)$ is the likelihood of Y_N given θ as defined in (27).
Finding the set of parameters given data, a model and prior distributions of parameters yielding the maximum of the posterior distribution is called maximum a posteriori (MAP).

4.1.4 Maximum a posteriori estimation

MAP estimation is an optimization approach seeking the parameter estimate that maximizes the posterior distribution [46]. Maximizing (30) then reduces to optimizing:

$$p(\theta, Y_N) \propto p(Y_N|\theta)p(\theta) \tag{31}$$

MAP estimation reduces to maximizing the likelihood function when the prior is a uniform distribution (i.e. $p(\theta)$ is constant), see (27) and (31). This indicates that ML is a special case of MAP. Also, the weaker a prior is (i.e. having a large standard deviation), the less difference there is between MAP estimation and ML. In general, one distinguishes between informative (highly peaked) and non-informative (not peaked) priors.

Introducing the following notation where σ_θ is a matrix with the prior standard deviations in the diagonal and R_θ is the prior correlation matrix:

$$\mu_\theta = E\{\theta\} \tag{32}$$
$$\Sigma_\theta = \sigma_\theta R_\theta \sigma_\theta = V\{\theta\} \tag{33}$$
$$\epsilon_\theta = \theta - \mu_\theta \tag{34}$$

Assuming that the priors all follow a Gaussian distribution, the posterior distribution can be rewritten as:

$$p(\theta|Y_N) \propto \left(\prod_{k=1}^{N} \frac{\exp\left(-\frac{1}{2}\epsilon_k^T R_{k|k-1}^{-1}\epsilon_k\right)}{\sqrt{\det(R_{k|k-1})}\left(\sqrt{2\pi}\right)^l} \right) p(y_0|\theta) \frac{\exp\left(-\frac{1}{2}\epsilon_\theta^T \Sigma_\theta^{-1}\epsilon_\theta\right)}{\sqrt{\det(\Sigma_\theta)}\left(\sqrt{2\pi}\right)^p} \tag{35}$$

Conditioning the posterior probability on y_0 and taking the negative logarithm gives:

$$-\log(p(\theta|Y_N, y_0)) \propto \frac{1}{2}\sum_{k=1}^{N}\left(\log(\det(R_{k|k-1})) + \epsilon_k^T R_{k|k-1}^{-1}\epsilon_k\right) + \frac{1}{2}\left(\left(\sum_{k=1}^{N} l\right) + p\right)\log(2\pi) + \frac{1}{2}\log(\det(\Sigma_\theta)) + \frac{1}{2}\epsilon_\theta^T \Sigma_\theta^{-1}\epsilon_\theta \tag{36}$$

The MAP solution is found by solving the nonlinear optimization problem:

$$\hat{\theta} = \arg\min_{\theta\in\Theta}\{-\log(p(\theta|Y_N, y_0))\} \tag{37}$$

This nonlinear optimization can be solved numerically through gradient-methods. Another method for finding the MAP solution is by using Markov Chain Monte Carlo (MCMC) simulations. MCMC is a brute force method that samples from the posterior distribution to create a rough shape of the posterior distribution and thereby estimates the MAP solution as implemented in WinBUGS [21, 26]. It is computationally time consuming because it can require thousands of samples before reaching convergence. On the contrary, gradient methods converge faster but suffer great difficulties if the objective function is noisy with local gradients not leading to a smaller value of the objective function.

4.1.5 Stochastic differential equations

Modelling a completely known physical system can be done using deterministic ordinary differential equations (ODEs) defined as

$$\frac{\mathrm{d}X}{\mathrm{dt}} = f(X(t), t) \tag{38}$$

$$y_k = X(t_k) + e_k \tag{39}$$

where $X(t)$ is the state of the system, $f()$ is the model, y_k is the discrete observations, and e_k is the measured errors, i.e. observation noise, assumed to be independent and identically distributed (i.i.d.) following a Gaussian distribution [47]. However, in biology one does not always know the true underlying system. In such cases, the discrepancies between the deterministic model and data from the physical system is composed of noise from two sources: measurement errors and systemic model errors. The magnitude of the systemic noise can be identified using stochastic differential equations (SDEs) defined as

$$\mathrm{d}x_t = f(x_t, u_t, t, \theta)\mathrm{d}t + \sigma(x_t, u_t, t, \theta)\mathrm{d}w_t \tag{40}$$

$$y_k = h(x_k, u_k, t_k, \theta) + e_k \tag{41}$$

The only difference between the ODE formulation in (38)-(39) and the SDE formulation in (40)-(41) is the diffusion term $\sigma(x_t, u_t, t, \theta)\mathrm{d}w_t$ corresponding to the system noise. Thus, solving an SDE with a very small value of σ is approximating solving an ODE. The term $f(x_t, u_t, t, \theta)\mathrm{d}t$ is called the drift and is the main process driving the system whereas the diffusion term is the system noise. Together, the drift and the diffusion describes the physical state of the system.

4.2 Application in CTSM-R

A team at the Technical University of Denmark (DTU) wrote a package for R allowing to do continuous time stochastic modelling (CTSM) [34,46]. The package was used to obtain the results in this report. This subsection focuses on how the mathematical concepts in the previous subsection are applied in CTSM-R.

4.2.1 Model structure

CTSM-R accepts Itô SDEs in the state space form as presented in (40)-(41). However, CTSM-R does not allow the system noise to depend directly on the state of the system [47], and thus (40) changes to

$$\mathrm{d}x_t = f(x_t, u_t, t, \theta)\mathrm{d}t + \sigma(u_t, t, \theta)\mathrm{d}w_t \tag{42}$$

Letting the system noise depend on the state can be mitigated in CTSM-R using a transformation of variables called the Lamperti transform [47, 48].
Although the nonlinear equations describing the model in (20)-(26) are presented as ODEs, they are implemented in CTSM-R as SDEs. The ODE presentation is chosen for simplicity.

4.2.2 Initial values

The CTSM-R environment is sensitive to the initial values of the states and thus good initial values are needed to converge to a solution within a reasonable number of iterations. When fitting the PD model, the initial value of the observed state was automatically identified in most datasets as the plasma glucose concentration at time 0. If the initial plasma glucose was not available in one dataset, the initial concentration in the same dog at the other dosing occasions were averaged and used as the initial value of the dataset missing an initial observation. Using the measured or averaged initial glucose concentration the model parameters did not converge to a solution in al datasets. In those cases the initial value was adjusted manually until convergence was reached.

4.2.3 Prior information

In the following all hyper-parameters are fixed, thus all prior probability distributions of parameters are fixed. The values of the hyper-parameters are determined from literature [15, 20] and listed in Table 4. All parameters are assumed positive. All parameters of the Hovorka part of the model are assumed to follow a log-normal distribution, except F_{01} which is normally distributed [21]. We also assume that E_0, E_{max}, EC_{50}, and γ follow normal distributions.
The insulin sensitivities in [20] were overestimated compared to the results of [21]. As pointed out in Section 2.4, dogs appear to be more sensitive to insulin than humans and thus the estimates listed in [20] are kept as prior information. However, the standard deviation in the logarithmic domain is doubled to allow a different distribution than in humans. The standard deviations of the parameters describing the effect of glucagon on GG are unknown and thus arbitrarily defined as 25% of the mean value estimated from literature [15].

Overall, the prior correlation matrix has the structure presented in Table 5. The correlations of the parameters describing the glucagon part of the model are unknown and thus defined as zero. The values of the prior correlation matrix are calculated from individual parameter fits [20] and presented in Table 6. Fixing one or more of the parameters in the PD model leads to removal of the corresponding parameter rows and columns from the correlation matrix.

Table 4: Prior distributions of PD model parameters listed with source as (mean, SD) in the fitted domain and 95% confidence interval in non-transformed domain calculated as $\exp(\text{mean} \pm 2 \cdot \text{SD})$ if log-transformed and as $\text{mean} \pm 2 \cdot \text{SD}$ if non-transformed, respectively.

Parameter	Source	Transformation	Prior distribution	95% confidence interval
k_{12}	[20]	log	(-2.82, 0.46)	[0.02-0.1]
k_{a1}	[20]	log	(-5.69, 1.12)	[0.0004-0.03]
k_{a2}	[20]	log	(-2.89, 0.70)	[0.01-0.2]
k_{a3}	[20]	log	(-3.74, 0.77)	[0.005-0.1]
S_T	[20]	log	(-5.48, 1.46)	[0.0002-0.08]
S_D	[20]	log	(-7.58, 2.34)	[$5{\cdot}10^{-6}$-0.05]
S_E	[20]	log	(-3.19, 1.74)	[0.001-1.3]
F_{01}	[20]	-	(9.68, 2.14)	[5.4-14]
E_0	Section 3.2.4	-	(8, 2)	[4-12]
E_{max}	Section 3.2.4	-	(72.1, 18)	[36-108]
EC_{50}	Section 3.2.4	-	(337.8, 85)	[168-508]
γ	Section 3.2.4	-	(1.25, 0.3)	[0.65-1.85]

Table 5: Overall structure of the full prior correlation matrix.

	k_{12}	k_{a1}	k_{a2}	k_{a3}	S_T	S_D	S_E	F_{01}	E_0	E_{max}	EC_{50}	γ
k_{12}	1	$\rho_{k_{12},k_{a1}}$		$\cdots$		$\cdots$		$\rho_{k_{12},F_{01}}$	0	$\cdots$	$\cdots$	0
k_{a1}	$\rho_{k_{a1},k_{12}}$	$\ddots$	$\ddots$						$\vdots$			$\vdots$
k_{a2}		$\ddots$						$\vdots$				
k_{a3}	$\vdots$			$\ddots$	$\ddots$				$\vdots$			$\vdots$
S_T				$\ddots$				$\vdots$				
S_D	$\vdots$					$\ddots$	$\ddots$		$\vdots$			$\vdots$
S_E						$\ddots$		$\rho_{S_E,F_{01}}$				
F_{01}	$\rho_{F_{01},k_{12}}$		$\cdots$		$\cdots$		ρ_{F_{01},S_E}	1	0			$\vdots$
E_0	0		$\cdots$		$\cdots$		$\cdots$	0	1	$\ddots$		
E_{max}	$\vdots$								$\ddots$	$\ddots$	$\ddots$	$\vdots$
EC_{50}	$\vdots$									$\ddots$	$\ddots$	0
γ	0	$\cdots$		$\cdots$		$\cdots$		$\cdots$		$\cdots$	0	1

Table 6: Values of the full prior correlation matrix.

	k_{12}	k_{a1}	k_{a2}	k_{a3}	S_T	S_D	S_E	F_{01}	E_0	E_{max}	EC_{50}	γ
k_{12}	1	0.73	-0.83	-0.14	0.27	0.46	0.22	0.07	0	0	0	0
k_{a1}		1	-0.97	-0.15	-0.23	-0.16	0.03	0.24	0	0	0	0
k_{a2}			1	0.08	0.20	0.05	0.08	-0.22	0	0	0	0
k_{a3}				1	-0.06	-0.16	-0.28	0.45	0	0	0	0
S_T					1	0.61	0.77	0.24	0	0	0	0
S_D						1	0.54	-0.51	0	0	0	0
S_E							1	0.02	0	0	0	0
F_{01}								1	0	0	0	0
E_0									1	0	0	0
E_{max}										1	0	0
EC_{50}											1	0
γ												1

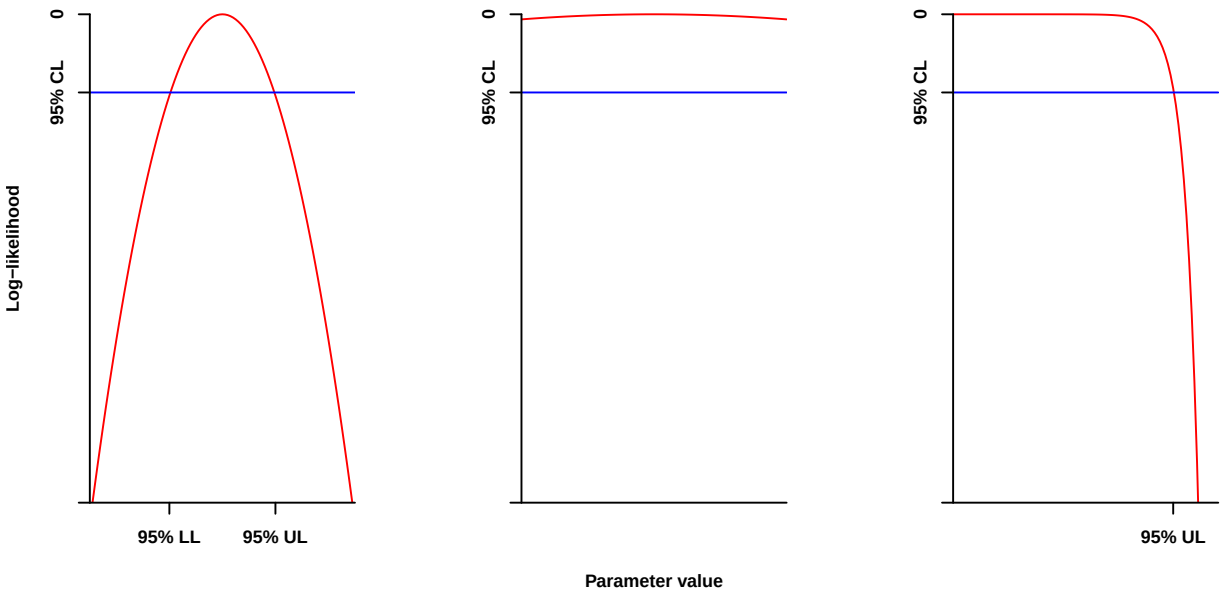

Figure 10: Theoretical examples of three types of profile likelihood plots; from left to right: highly peaked (identifiable), flat (structural non-identifiable), and asymmetric (practical non-identifiable). The 95% confidence limit (CL) is blue. The x-axis shows the 95% lower limit (LL) and upper limit (UL) of the parameter value.

4.2.4 Parameter identifiability

We have performed profile likelihood analysis of each model parameter using graphical presentation to investigate which model parameters are identifiable, see Figure 10 for examples of profile log-likelihood plots. A profile log-likelihood with values only exceeding the 95% confidence limit for the entire physiological range of a parameter indicates that the parameter is not structural identifiable, i.e. if the profile likelihood is flat, the parameter value does not influence the maximum achievable likelihood in fitting the dataset and might as well be fixed. To improve the parameter estimates of the remaining parameters, the unidentifiable parameters were fixed at their prior mean values. On the contrary, if a profile likelihood is highly peaked, the parameter is identifiable and should not be fixed. When a profile likelihood is asymmetric with either no upper or lower limit as seen in Figure 10 at the right, the parameter value is not practically identifiable and could also be fixed if the prior mean value is included in the 95% confidence interval. However, having a prior distribution it is not necessary to fix a parameter with an asymmetric profile log-likelihood but could increase the certainty of the remaining parameters.
As the calculation of a profile likelihood is very time consuming due to optimization of the remaining parameters for each fixed parameter value, the profile log-likelihood plots are initially very coarse with only few points. Profiles are refined as unidentifiable parameters are fixed and calculations are speeding up. Ideally, one should continue the cycle of fixing unidentifiable parameters until all remaining parameters are identifiable. In this study, we have only carried out five cycles of profile likelihood analysis. More parameters could possibly be fixed without changing the likelihood of the model fit significantly. Fitting a model containing unidentifiable parameters using MAP estimation is not wrong, but it comes at the expense of larger confidence intervals of the remaining parameters. The fitted values of parameters having flat or asymmetric profile likelihoods i.e. unidentifiable parameters will mainly be determined by the prior parameter distributions and less determined by data.

4.2.5 Model fitting and validation

Each PK dataset was fitted separately by ML using ODEs by fixing the system noise terms at small values. Since the PK model will be used for simulations we seek the ODE solution instead of the SDE solution. The basal concentration of glucagon was sought estimated. However, the basal level for the analogue was defined as zero and thus not estimated.

Each PD dataset was fitted separately by MAP with the priors listed in Table 4 and the correlation matrix displayed in Table 6. The parameters of each dataset were identified separately based on prior information rather than a population model. All parameters of the Hovorka model except F_{01} were fitted in the logarithmic domain as they are assumed to follow a log-normal distribution [21]. Moreover, all parameters were assumed to be positive. When dealing with small values like the transfer rate constants and sensitivities, log-transformation of the parameters ensure that they are always positive.

During the profile likelihood analysis the PD model was fitted as ODEs. After several model parameters were fixed we fitted the model using SDEs. However, since equations (21) and (24)-(26) were validated by tracer data in a previous publication [20], we fixed the diffusion terms of these states to small values and considered the equations as ODEs. The only modified and thus non-validated state was equation (20) and thus we estimated the diffusion term thereof. As described in Kristensen et al. [33], to validate the model structure, the model was first fitted using SDEs and if the diffusion term was insignificant, i.e. having a large p-value, the model was fitted again using ODEs to obtain the final parameter estimates for simulation purposes. However, if the diffusion term was not insignificant the model structure was incorrect [33]. The necessity of each of the varying model parameters was confirmed by significant p-values less than 0.05.

Furthermore, the model validity was investigated by residual analysis. Residuals should ideally be i.i.d. which was examined by plotting the residuals as a function of time and by plotting the autocorrelation function (ACF). The residuals plot can reveal if there is a drift or change in variance of the residuals over time i.e. if they are identically distributed. The ACF can reveal if there is a pattern in the residuals showing correlation between residuals at different lags i.e. if they are independent [49]. Moreover, very large values of the ACF exceeding the confidence limit imply that the model is not describing the data well.

Simulations of the mean prediction and standard deviations are carried out using extended Kalman filter without updating the states [34]. Predicting future values in a system with very little system noise and thus no updating corresponds to deterministic simulation.
It is however possible to perform stochastic simulations in CTSM-R by adding system noise to simulate real life experimental data [34]. Each realization of the stochastic process will be slightly different from another although determined by the size of the noise terms. We can interpret the actual data used for model fitting as one realization of the underlying stochastic process.

5 Results

Despite CTSM-R uses a robust estimation method [46], extreme outliers can largely impact the fit when the number of observations is small. Fitting of the PK data to the simple model was mostly robust to outliers. However, one PK datapoint as listed in Table 3 was so extreme that removing it greatly changed and improved the fit.
The PD model was more sensitive to outliers in both the input data and in the observations due to the large number of model parameters compared to number of observations. Six glucose observations appeared to be outliers as listed in Table 3. Due to the number of model parameters, the glucose observations had to

Table 7: Fitted or fixed PK model parameters (mean, SD). *Non significant. $^{\triangle}$Fixed.

Parameter	Unit	Glucagon	ZP-GA-1
k_1	min^{-1}	(0.134, 0.077)	(0.125, 0.072)
k_2	min^{-1}	(0.0159, 0.0048)	(0.0116, 0.0031)
Cl	mL/kg/min	(56.9, 13.2)	(88.5, 18.8)
C_b	pg/mL	0*	$0^{\triangle}$

Table 8: PK endpoints extracted from PK model fits (mean, SD).

PK endpoint	Unit	Dose level	Glucagon	ZP-GA-1
T_{max}	min	low	(23.9, 11.4)	(25.3, 9.4)
		high	(19.3, 5.4)	(22.4, 6.6)
C_{max}/Dose	nmol/L per nmol/kg	low	(0.059, 0.018)	(0.043, 0.010)
		high	(0.097, 0.017)	(0.059, 0.010)

be replaced by linear interpolation to maintain an identifiable model.

5.1 PK

5.1.1 Parameter estimates

Table 7 lists the average and standard deviation of the PK model parameters for each drug over the populations. As mentioned in section 2.4, it was not possible to measure low glucagon concentrations in any datasets. Due to this lack of data at low concentrations, it was not possible to estimate basal glucagon concentration in plasma.
The PK model fit is used as an input to the following PD model fitting and could also be used for simulation purposes.

5.1.2 PK Model fits

After fitting the PK model to data, relevant endpoints were extracted from the fits and presented in Table 8. Paired t-tests of the surrogate marker for onset of action, T_{max}, showed no difference between ZP-GA-1 and glucagon (p-value = 0.3).
C_{max} is significantly different for ZP-GA-1 compared to glucagon (p-value = 0.006).
Figure 11 displays examples of PK model fits with 95% confidence limits of the simulation both with regular and logarithmic base-10 y-axes ($\log_{10}$). Figures 21-25 in Appendix B shows all PK fits.

5.2 PD

A few model building cycles have been carried out. The following sections only show results of the last and final model. However, the sections will refer qualitatively to observations made during the model building cycle to justify the decisions made by the model builder.

5.2.1 Reducing variables

Having a large model with twelve parameters and observation noise, some parameters had to be fixed to increase the certainty of other model parameters. To investigate which model parameters were unidentifi-

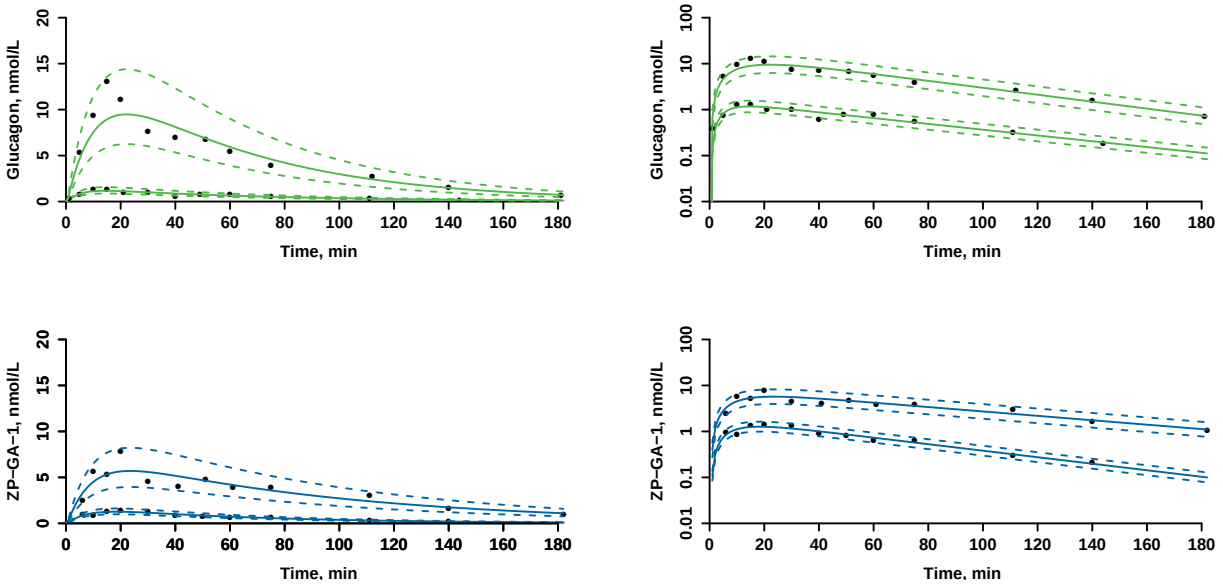

Figure 11: PK responses to low and high doses of glucagon and ZP-GA-1 in dog 3. Left graphs are with regular y-axes and right graphs are with logarithmic base-10 y-axes ($\log_{10}$).

able, we plotted profile likelihoods of all parameters for each dataset. Figure 12a shows an example from the first cycle of profile likelihood analysis in one dataset. After the first cycle one parameter with a flat profile likelihood was fixed, and another cycle of profile likelihood analysis was carried out. These cycles continued until a total of four parameters were fixed at their prior mean values: k_{a2}, E_0, EC_{50}, and γ. However, γ was fixed at 1 since this reduced the model complexity and makes biologic sense. Figure 12b shows an example from the last cycle of profile likelihood analysis in the same dataset as above.
The reduction of variables is justified by reasoning regarding model structure and input dynamics. E_0 corresponding to GN can not be identified due to the model structure i.e. subtraction from E_{max}. The two parameters determining the curvature of the GG response to glucagon, EC_{50} and γ, can not be determined due to input dynamics. As previously mentioned, most dogs had very high plasma concentrations of glucagon or analogue during the entire study time and we therefore expect the GG response to be saturated at all times. Not having data with low glucagon concentrations makes it impossible to determine these parameters describing the response at low glucagon concentrations.
Unidentifiability of k_{a2} is likely due to the model structure since the parameter describes the insulin transfer that affects the glucose disposal of the non-accessible compartment. Determining the influence of insulin on glucose disposal requires tracer data which is not available.

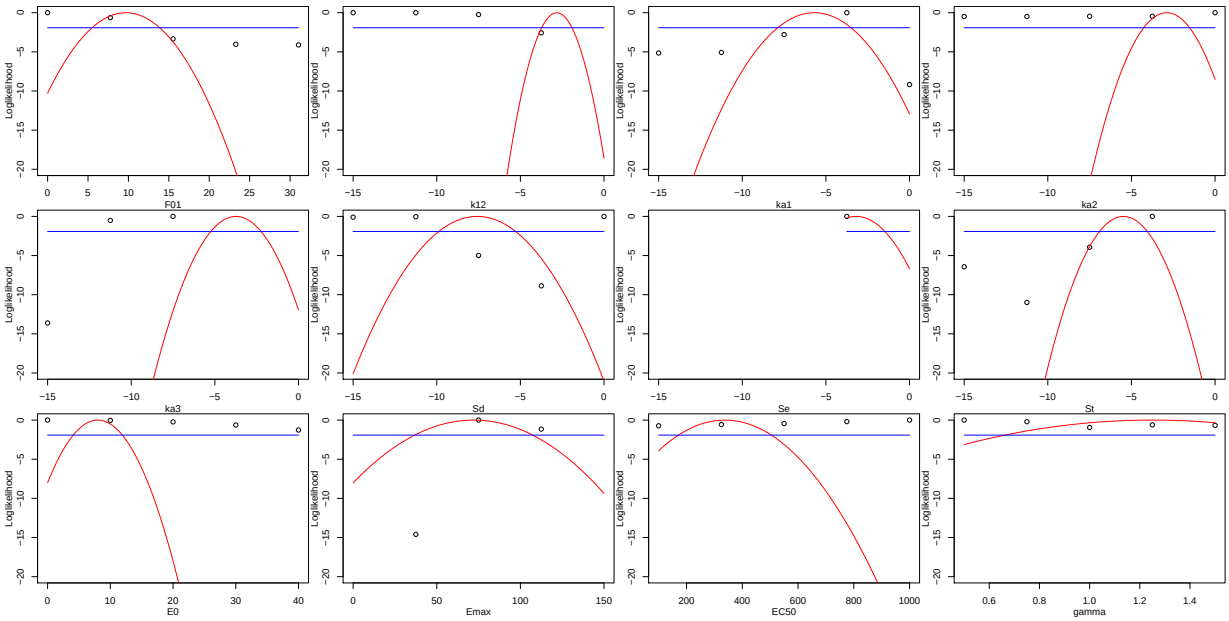

(a) Initial profile likelihoods when no parameters are fixed.

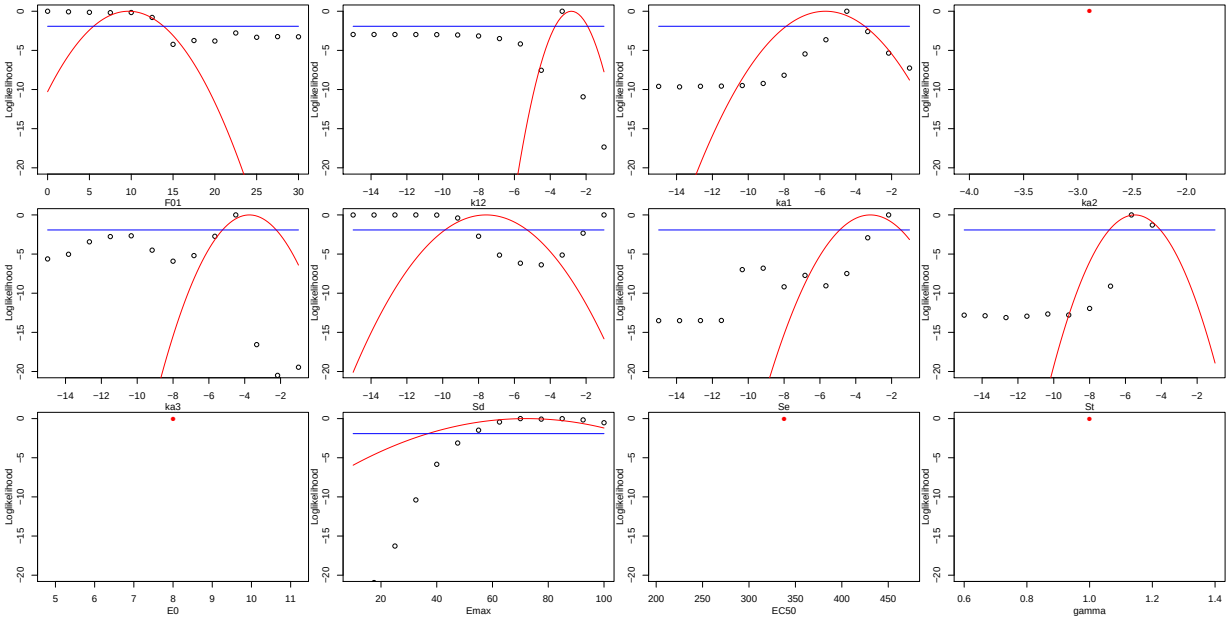

(b) Fourth iteration of profile likelihood analysis when four parameters are fixed.

Figure 12: Profile likelihoods of all twelve model parameters in dog 3 after high dose of glucagon. Red points illustrate fixed parameter values. Red curves illustrate prior parameter distributions. Horizontal blue lines are 95% confidence limits of parameter values.

Table 9: Ratio of datasets with significant p-values less than 0.05 corresponding to 95% confidence level when estimated in SE setting versus OE setting. P-values of fixed parameters do not exist but the parameters are included in the table for completeness.

	Glucagon		ZP-GA-1	
Parameter	SE	OE	SE	OE
k_{12}	10/10	10/10	10/10	10/10
k_{a1}	10/10	10/10	10/10	10/10
k_{a2}			-	
k_{a3}	10/10	10/10	10/10	10/10
S_T	10/10	10/10	10/10	10/10
S_D	10/10	10/10	10/10	10/10
S_E	10/10	10/10	10/10	10/10
F_{01}	10/10	10/10	10/10	10/10
E_0			-	
E_{max}	7/10	10/10	9/10	10/10
EC_{50}			-	
γ			-	
σ_1	0/10	-	0/10	-

As an example, the increase in certainty of parameter value when reducing the number of variables is graphically evident for k_{a1} in Figure 12. At the initial cycle the 95% confidence interval of the logarithm of the parameter is approximately [-7 to -3], but reduces to [-5 to -3.5] when four parameters are fixed. Same tendency can be observed for other model parameters.

5.2.2 Model validity

After reduction of variables using profile likelihood analysis we investigate using SDEs if the model describes the physiological system adequately i.e. if the model has insignificant system noise. As previously argued, we only examine the noise of equation (20). Table 9 lists the proportion of datasets with significant p-values for each PD model parameter with and without the coefficient of the diffusion term, σ_1, for both of the compounds. Using SDEs we observe that the model parameters are significant at a 5% confidence level in the majority of datasets and that the diffusion coefficient is insignificant in all datasets. σ_1 is then fixed at a small value and the PD model parameters re-estimated using ODEs. After fixing σ_1, all model parameters are significant in all datasets. We can not reject that the model describes the underlying physiological system.

5.2.3 Residual Analysis

After the final estimation of PD model parameters using ODEs we analyse the standardized residuals to verify the quality of the model in describing data. Figure 13 shows an example of the standardized residuals plot and ACF showing i.i.d. residuals thus no trends in residuals and no significant correlation between residuals.

However, dealing with data having very few observations makes it challenging to be strict to the rules of i.i.d. residuals. Especially the residuals plot is difficult to interpret in most cases due to few observations. The ACF also has some limitations in that data was not equidistantly sampled. Most ACF are

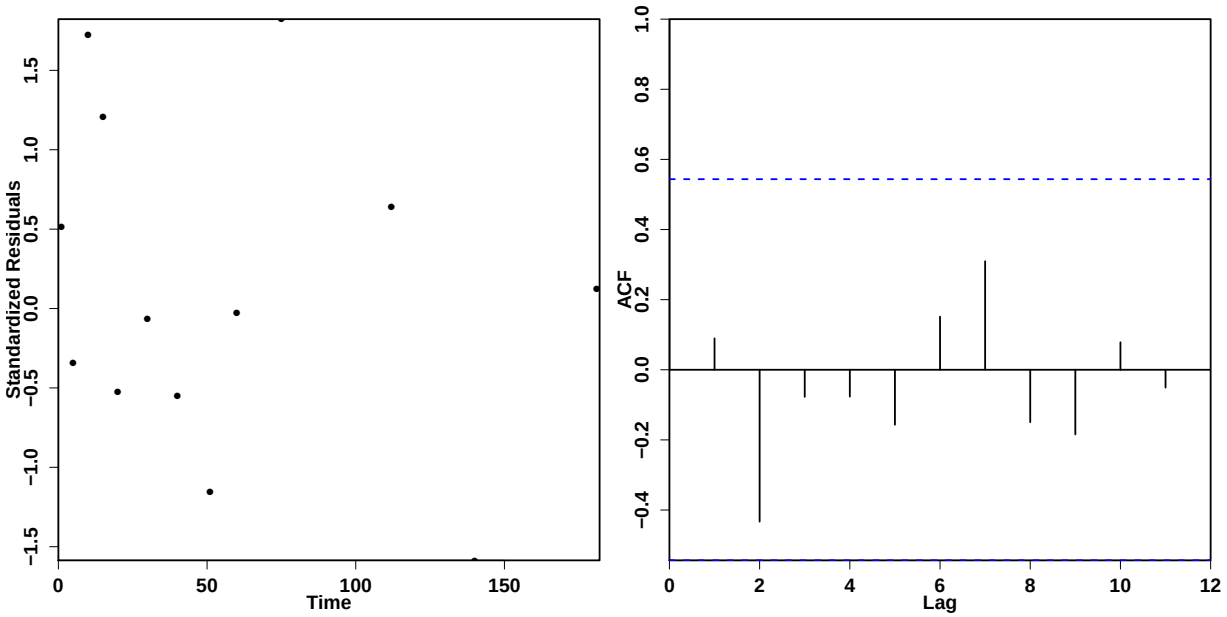

Figure 13: Example of standardized residuals plot and ACF of residuals of model fit to dataset from dog 3 after high dose of glucagon.

within the confidence limits.
Based on the residual analysis the model describes the dynamics in the data well.

5.2.4 PD Model fits

In Section 5.2.1 we reduced the number of PD model parameters by removing unidentifiable parameters. In Section 5.2.2 we described how the model structure is sufficient to capture the dynamics of the physical system. In Section 5.2.3 we confirmed that the fit did not give rise to trends in the residuals. Finally, we can verify that the model is satisfactory based on visual inspection of the PD model fit together with data. Figure 14 presents examples of PD model fits together with model inputs after administration of glucagon at low and high dose levels in one dog. In the two examples, the model is fitting data well with narrow confidence limits around the simulation. Within 100 minutes we observe a peak in glucose concentration and a return to baseline. At the end of the sampling period the glucose concentrations show a tendency to rise slowly.
Figure 15 presents examples of PD model fits together with model inputs after administration of ZP-GA-1 at low and high dose levels in one dog. The trends in data and the PD model fits are similar to the ones after administration of glucagon described above.
Figures 26-30 in Appendix C present all PD model fits.

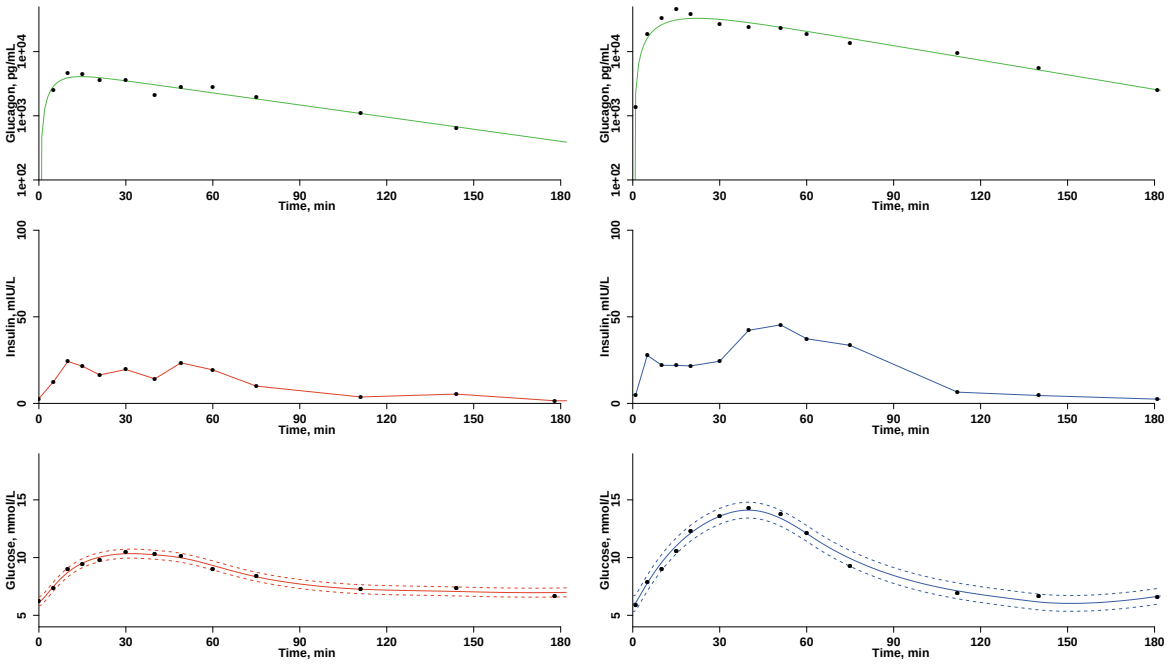

(a) Dog 3, 20 nmol/kg.

(b) Dog 3, 120 nmol/kg.

Figure 14: Plasma concentrations of PD model inputs glucagon and insulin together with PD model fit of glucose after administration of glucagon.

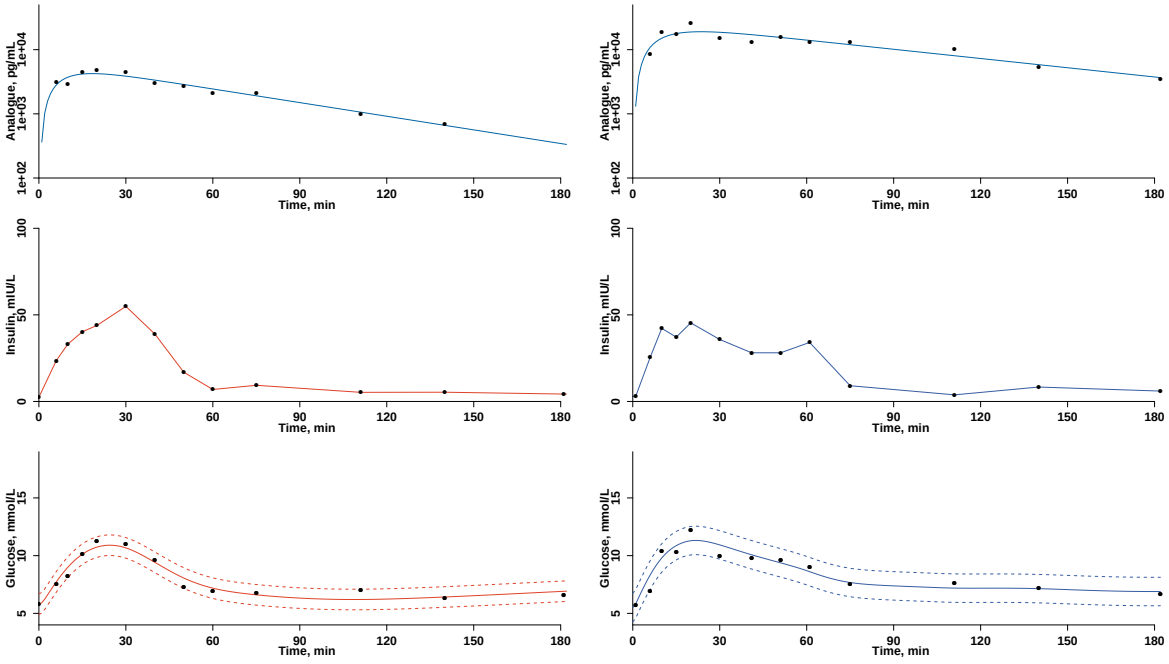

(a) Dog 3, 20 nmol/kg.

(b) Dog 3, 120 nmol/kg.

Figure 15: Plasma concentrations of PD model inputs ZP-GA-1 and insulin together with PD model fit of glucose after administration of ZP-GA-1.

Table 10: Posterior distributions of PD model parameters for the population in fitted domain reported as (mean, SD). Parameters not in parenthesis are fixed.

Parameter	Glucagon	ZP-GA-1
$\log(k_{12})$	(-2.87, 0.27)	(-3.02, 0.23)
$\log(k_{a1})$	(-5.19, 0.86)	(-5.90, 0.83)
$\log(k_{a2})$	-2.89	-2.89
$\log(k_{a3})$	(-4.88, 0.73)	(-4.70, 0.98)
$\log(S_T)$	(-5.65, 0.86)	(-5.35, 0.50)
$\log(S_D)$	(-9.11, 0.93)	(-8.72, 1.15)
$\log(S_E)$	(-2.71, 0.57)	(-2.95, 0.43)
F_{01}	(9.8, 1.5)	(9.6, 2.0)
E_0	8	8
E_{max}	(50.1, 13.7)	(53.8, 16.5)
EC_{50}	337.8	337.8
γ	1	1

5.2.5 Parameter estimates

We assume that the variations in parameters within dogs are negligible compared to the variations between dogs. As prior information we used Gaussian distributions and using the individually fitted parameters we can calculate similar posterior distributions of PD model parameters.
Table 10 lists the posterior distributions of each parameter separated by drug and study for the population of dogs. During the PK analysis we noticed that the onset of action and maximum concentration of glucagon were different between the studies. We therefore separate the parameters of the two studies in this analysis, too. During estimation, most parameters are log-transformed.
For ease of comparison to values reported in literature [20], the averages of the log-transformed parameters are transformed back and listed together with ranges in Table 11. Fixed parameters are listed for completeness in both tables.
Table 12 shows the posterior correlation matrix of both PK and PD model parameters.
The following Section describes observations related to these posterior distributions and correlations.

Table 11: Average of PD model parameters in normal domain together with range. Fixed parameters are listed for completeness.

Parameter	Glucagon	ZP-GA-1
k_{12}	0.057 (0.038-0.085)	0.049 (0.033-0.081)
k_{a1}	0.0056 (0.0019-0.0279)	0.0027 (0.0009-0.0192)
k_{a2}	0.055	0.055
k_{a3}	0.0076 (0.0038-0.0508)	0.0091 (0.0038-0.0657)
$S_T \cdot 10^{-4}$	35 (13-117)	48 (27-110)
$S_D \cdot 10^{-4}$	1.1 (0.2-3.8)	1.6 (0.6-35.8)
$S_E \cdot 10^{-4}$	666 (178-1323)	523 (281-892)
F_{01}	9.8 (8.0-13.1)	9.6 (5.3-12.3)
E_0	8	8
E_{max}	50.1 (26.6-73.2)	53.8 (24.1-71.8)
EC_{50}	337.8	337.8
γ	1	1

Table 12: Posterior correlation matrix of PK and PD model parameters and body weight.

	k_1	k_2	Cl	w	$\log(k_{12})$	$\log(k_{a1})$	$\log(k_{a3})$	$\log(S_T)$	$\log(S_D)$	$\log(S_E)$	F_{01}	E_{max}
k_1	1	0.26	0.33	-0.54	-0.08	-0.25	0.49	0.52	-0.01	-0.13	0.50	-0.55
k_2		1	-0.27	-0.24	0.34	0.17	0.12	0.16	-0.03	-0.11	0.27	0.04
Cl			1	-0.51	-0.37	-0.55	0.44	0.60	0.11	-0.22	0.35	-0.10
w				1	0.10	0.32	-0.46	-0.63	0.02	0.19	-0.55	0.25
$\log(k_{12})$					1	0.78	-0.13	-0.21	0.02	0.01	0.11	0.09
$\log(k_{a1})$						1	-0.45	-0.68	-0.44	0.31	-0.07	0.18
$\log(k_{a3})$							1	0.60	0.00	-0.80	0.78	-0.59
$\log(S_T)$								1	0.36	-0.32	0.53	-0.19
$\log(S_D)$									1	0.00	-0.45	0.04
$\log(S_E)$										1	-0.57	0.40
F_{01}											1	-0.40
E_{max}												1

Table 13: P-values of two-tailed paired t-tests comparing PD model parameter estimates of glucagon versus analogue within study.

Parameter	Glucagon vs. ZP-GA-1
k_{12}	0.29
k_{a1}	0.09
k_{a2}	-
k_{a3}	0.42
S_T	0.19
S_D	0.42
S_E	0.14
F_{01}	0.81
E_0	-
E_{max}	0.51
EC_{50}	-
γ	-

5.2.6 Native glucagon versus glucagon analogue

The reason for doing cross-over studies of glucagon and the glucagon analogue is to be able to compare the dynamics of the compounds without too many confounding factors like biological variations. Table 13 presents p-values of paired t-tests between glucagon and the glucagon analogue. No model parameters are significantly different on a 5% confidence level.

6 Discussion

In this report, we present a novel model describing how insulin and glucagon contribute to the EGP in dogs. The model is based on physiological knowledge and parameter estimates are based on data from pre-clinical studies in five dogs. The PD model description is contentious compared to most existing models in several ways: claiming that GG is completely suppressed when insulin concentration exceeds a threshold as in Hovorka et al. [20], claiming that GG saturates when glucagon concentration is high, and claiming a multiplicative effect of insulin and glucagon as in Emami et al. [26]. Moreover, we have used the model to compare PD characteristics of marketed glucagon and a novel glucagon analogue invented by Zealand Pharma A/S.

According to our PD model there exists a certain threshold of insulin concentration at which the GG is completely suppressed. From equation (22) the threshold can easily be identified using the insulin sensitivity on GG as S_E^{-1}. Using the average parameter estimate listed in Table 11 we find a threshold of less than 20 mIU/L. This threshold is considerably lower than the threshold identified by Cherrington as 45 mIU/L [15]. Also, El Youssef et al. found that insulin concentrations exceeding 40 mIU/L only results in EGP of roughly 20 mg/kg during 60 minutes [28]. This EGP production of $\sim$0.33 mg/kg/min is similar magnitude as GN of $\sim$0.5 mg/kg/min observed by Cherrington [15]. Thus, the results by El Youssef et al. at insulin concentrations exceeding 40 mIU/L could be explained by insulin's suppression of GG.
The human prior of S_E suggested an insulin threshold of 19 mIU/L [20], whereas a later publication suggested an average insulin threshold of 85 mIU/L based on the value of S_E [21]. However, both of these

estimates of S_E were based on human data. As discussed in Section 2.4 dogs have lower basal insulin levels than humans and are therefore more sensitive to insulin than humans. It is thus reasonable that the threshold at which the GG is completely suppressed is lower in dogs than in humans.
The graphs of raw data in Appendix A reveal that the dog's insulin concentrations exceed even the human threshold of GG suppression during at large parts of the study time. In some datasets we notice a slight increase in blood glucose concentrations during the last part of the study which could be explained by GG no longer being suppressed by insulin and a plasma glucagon concentration that is still much higher than basal levels. However, we only observe this slight increase in plasma glucose in some datasets. This could be explained by the delay in insulin action on plasma glucose described by the small rate constant with a half-life of approximately 90 minutes which corresponds to the remaining of the sampling period after plasma insulin concentrations have returned to baseline.

The diabetes community is speculating whether glucagon works when insulin inhibits GG. El Youssef et al. found in diabetes patients that increasing glucagon doses of 25-175 μg increases EGP at insulin concentrations less than 30 mIU/L [28], but increasing doses up to 175 μg have no effect on EGP at insulin concentrations exceeding 40 mIU/L as explained previously. Blauw et al. investigated the glucose response in patients with diabetes to various doses of glucagon from 0.1-1 mg at different blood glucose levels and concluded that blood glucose level was irrelevant to the glucose response to glucagon [50]. Unfortunately, the study does not report insulin concentrations. Ranjan et al. investigated the glucose response in diabetes patients to glucagon doses of 100-300 μg at insulin concentrations of 8-20 mIU/L and found no significant increase in glucose response after a glucagon dose of 300 μg compared to 200 μg [51]. A study by Graf et al. in healthy showed no further effect size of glucagon doses larger than 250 μg [52]. The studies by Ranjan et al. and Graf et al. suggest a saturation effect of glucagon in both healthy and patients with diabetes.
The glucagon doses used in the pre-clinical dog study ranged 20-120 nmol/kg (0.07-0.4 mg/kg) corresponding to human equivalent doses of 0.04-0.2 mg/kg using allometric scaling. Thus, the previous studies suggesting a saturation effect of glucagon doses exceeding 0.2 mg supports our observations that the glucose responses of the dogs were saturated at all dose levels.
According to Cherrington the GG response to glucagon is almost saturated for glucagon concentrations exceeding approximately 1000 pg/mL [15]. From the graphs of raw data in Figures 16-20 we observe that plasma glucagon concentrations are higher than 1000 pg/mL most of the study duration. We only have very limited data when glucagon concentrations are low. During the reduction of variables we recognized this fact since we were not able to identify the parameters describing GG response to glucagon at low concentrations, but only at saturated concentrations. We still believe that the sigmoid E_{max} model presented here is valid in describing the effect of glucagon on GG because it builds on knowledge from literature in particular Cherrington [15]. Moreover, we believe that this novel model is more physiologically correct than previous models based on the minimal model or a linear approximation since these models do not describe the saturation effect of glucagon on GG [24–26]. Future studies should be designed so that the plasma glucagon concentration does not yield saturated EGP response for the entire study duration.

The multiplicative effect of insulin and glucagon on GG was proposed by Emami et al. [26]. The idea was derived from Hovorka et al. who states that with increasing insulin concentration the total EGP decreases linearly [20]. The model by Emami et al. multiplies the effect of insulin as described by Hovorka et al. with an expression stating that GG increases linearly when glucagon increases.
In this report, we have extended the model by Emami et al. to include saturation of glucagon. As the glucose response to glucagon was saturated during the entire study time for most datasets, the sophisticated sigmoid E_{max} model practically reduces to a constant value and thus the expression for GG originally

proposed by Hovorka et al.

Despite the saturated GG response due to glucagon, the model assumes that the glucogen stores in the liver are never depleted. As the study was conducted over short time, this is a fair assumption. Moreover, the glucose response from breakdown of glycogen is suppressed by insulin most of the study time. Recent data shows that small frequent glucagon boluses do not deplete the glucogen stores [22]. The study by Castle et al. has a few limitations in that it was carried out over short time and all participant were well-fed and had good control of their diabetes. It is however especially the poorly controlled patients that would need the glucagon bolus regularly. The effects of repeated daily and long term use of glucagon remain unknown. Studies investigating the long term effects are needed to verify that the glucose response to glucagon does not change over time.

The used datasets posed other challenges than not covering low glucagon concentrations. The study was not optimal for the purpose of fitting models describing the glucose-insulin-glucagon dynamics nor designed for identifying how insulin and glucagon affect EGP. The datasets were sparsely sampled which made it necessary to fix some parameters in order to increase the certainty of the estimates of the remaining parameters. We used profile likelihood analysis to justify fixation of four PD model parameters. Residual analysis of time series with only 14 observations is challenging and should not be considered as strict as an analysis using ten times the number of observations. Not all residuals plot and ACFs showed i.i.d. but visual inspection of model fits confirmed that the model described data well for the purpose of simulation.
We chose not to do cross-validation of the model, as this would be a waste of our limited amount of data. Also, with inter and intra biological variation, we would not expect to get good PD model fits testing parameters estimated in one dataset in another. Only in cases with constant conditions can such cross validation methods lead to meaningful and fair results.

In this report we focused on fitting data from individual trials using prior information in order to obtain a model suitable for simulation of the glucose-insulin-glucagon dynamics. The posterior parameter distributions and correlation matrix form a population from which a parameter set can be sampled for simulation of a subject. The estimated model parameters depend on the prior parameter distributions to some extend. However, comparing the prior parameter distributions in Table 4 with the posterior parameter distributions in Table 10, we observe that most posterior distributions are much narrower than the initial prior distributions of parameters, i.e. the parameter distributions are more informative.
The parameter estimation could be re-done by performing population modelling thus determining, not only the individual model parameters, but the hyper-parameters, i.e. population parameters, too. We also expect this simulation model to be valid in describing human glucose-insulin-glucagon dynamics although possibly with different population parameter distributions and parameter correlations.

We used a simple PK model together with the novel PD model to compare glucagon with a novel glucagon analogue referred to as ZP-GA-1 invented by Zealand Pharma A/S. Comparing PK between compounds, we did not find any significant differences for ZP-GA-1 compared to glucagon. However, we did find a significantly higher peak concentration of the analogue compared to glucagon. This is in agreement with the higher bioavailability of the analogue compared to glucagon, see Table 2 in Section 2.2. Comparing PD model parameters between glucagon and the analogue we did not find any significant differences at a 95% confidence level. Therefore, we can not reject that the analogue has similar PD effect on the glucose response and has similar PK characteristics to marketed glucagon.

In conclusion, we developed a novel model of the complex glucose-insulin-glucagon dynamics based on physiology and data. We demonstrated that the model describes the glucoregulatory system well and enables simulations of glucose dynamics knowing insulin and glucagon plasma concentrations.
Comparisons of marketed glucagon with the novel glucagon analogue did not show any differences in PK or PD characteristics.
This report presents parameter estimates for simulations of the glucose-insulin-glucagon dynamics in dogs but could be extended to simulations of the human dynamics after obtaining parameter estimates based on similar studies in humans.

References

[1] R. Hovorka, "Closed-loop insulin delivery: from bench to clinical practice," *Nature Reviews Endocrinology*, vol. 7, no. 7, pp. 385–395, 2011.

[2] S. J. Russell, F. H. El-Khatib, D. M. Nathan, K. L. Magyar, J. Jiang, and E. R. Damiano, "Blood glucose control in type 1 diabetes with a bihormonal bionic endocrine pancreas," *Diabetes Care*, vol. 35, no. 11, pp. 2148–2155, 2012.

[3] S. J. Russell, F. H. El-Khatib, M. Sinha, K. L. Magyar, K. McKeon, L. G. Goergen, C. Balliro, M. A. Hillard, D. M. Nathan, and E. R. Damiano, "Outpatient glycemic control with a bionic pancreas in type 1 diabetes," *The New England Journal of Medicine*, vol. 371, no. 4, pp. 313–325, 2014.

[4] S. J. Russell, M. A. Hillard, C. Balliro, K. L. Magyar, R. Selagamsetty, M. Sinha, K. Grennan, D. Mondesir, L. Ehklaspour, H. Zheng, E. R. Damiano, and F. H. El-Khatib, "Day and night glycaemic control with a bionic pancreas versus conventional insulin pump therapy in preadolescent children with type 1 diabetes: a randomised crossover trial," *The Lancet Diabetes & Endocrinology*, vol. 4, pp. 233–243, 2016.

[5] A. Haidar, L. Legault, M. Dallaire, A. Alkhateeb, A. Coriati, V. Messier, P. Cheng, M. Millette, B. Boulet, and R. Rabasa-Lhoret, "Glucose-responsive insulin and glucagon delivery (dual-hormone artificial pancreas) in adults with type 1 diabetes: a randomized crossover controlled trial," *Canadian Medical Association Journal*, vol. 185, no. 4, pp. 297–305, 2013.

[6] A. Haidar, L. Legault, L. Matteau-Pelletier, V. Messier, M. Dallaire, M. Ladouceur, and R. Rabasa-Lhoret, "Outpatient overnight glucose control with dual-hormone artificial pancreas, single-hormone artificial pancreas, or conventional insulin pump therapy in children and adolescents with type 1 diabetes: an open-label, randomised controlled trial," *The Lancet Diabetes & Endocrinology*, vol. 3, no. 8, pp. 595–604, 2015.

[7] A. Haidar, L. Legault, V. Messier, T. M. Mitre, C. Leroux, and R. Rabasa-Lhoret, "Comparison of dual-hormone artificial pancreas, single-hormone artificial pancreas, and conventional insulin pump therapy for glycaemic control in patients with type 1 diabetes: an open-label randomised controlled crossover trial," *The Lancet Diabetes & Endocrinology*, vol. 3, no. 1, pp. 17–26, 2015.

[8] V. Gingras, R. Rabasa-Lhoret, V. Messier, M. Ladouceur, L. Legault, and A. Haidar, "Efficacy of dual-hormone artificial pancreas to alleviate the carbohydrate-counting burden of type 1 diabetes: A randomized crossover trial," *Diabetes & Metabolism*, vol. 42, pp. 47–54, 2015.

[9] J. R. Castle, J. M. Engle, J. El Youssef, R. G. Massoud, K. C. J. Yuen, R. Kagan, and W. K. Ward, "Novel use of glucagon in a closed-loop system for prevention of hypoglycemia in type 1 diabetes," *Diabetes Care*, vol. 33, no. 6, pp. 1282–1287, 2010.

[10] J. El Youssef, J. R. Castle, D. L. Branigan, R. G. Massoud, M. E. Breen, P. G. Jacobs, B. W. Bequette, and W. K. Ward, "A controlled study of the effectiveness of an adaptive closed-loop algorithm to minimize corticosteroid-induced stress hyperglycemia in type 1 diabetes," *Journal of diabetes science and technology*, vol. 5, no. 6, pp. 1312–1326, 2011.

[11] A. C. van Bon, J. Hermanides, R. Koops, J. B. L. Hoekstra, and J. H. DeVries, "Postprandial glycemic excursions with the use of a closed-loop platform in subjects with type 1 diabetes: a pilot study," *Journal of diabetes science and technology*, vol. 4, no. 4, pp. 923–928, 2010.

[12] A. C. van Bon, L. D. Jonker, R. Koebrugge, R. Koops, J. B. L. Hoekstra, and J. H. DeVries, "Feasibility of a bihormonal closed-loop system to control postexercise and postprandial glucose excursions," *Journal of diabetes science and technology*, vol. 6, no. 5, pp. 1114–1122, 2012.

[13] A. C. van Bon, Y. M. Luijf, R. Koebrugge, R. Koops, J. B. L. Hoekstra, and J. H. DeVries, "Feasibility of a portable bihormonal closed-loop system to control glucose excursions at home under free-living conditions for 48 hours," *Diabetes technology & therapeutics*, vol. 16, no. 3, pp. 131–136, 2014.

[14] H. Blauw, A. C. van Bon, R. Koops, and J. H. DeVries, "Performance and safety of an integrated bihormonal artificial pancreas for fully automated glucose control at home," *Diabetes, Obesity and Metabolism*, 2016.

[15] A. D. Cherrington, "Control of glucose production in vivo by insulin and glucagon," in *Comprehensive Physiology 2011, Supplement 21: Handbook of Physiology, The Endocrine System, The Endocrine Pancreas and Regulation of Metabolism*, First published in print 2001, pp. 759–785.

[16] Novo Nordisk A/S. (2015) GlucaGen (glucagon [rdna origin] for injection) patient information. [Online]. Available: http://www.novo-pi.com/glucagenhypokit.pdf

[17] Eli Lilly and Company. (2012) Information for the physician - glucagon for injection (rdna origin). [Online]. Available: http://pi.lilly.com/us/rglucagon-pi.pdf

[18] B. Newswanger, S. Ammons, N. Phadnis, W. K. Ward, J. Castle, R. W. Campbell, and S. J. Prestrelski, "Development of a highly stable, nonaqueous glucagon formulation for delivery via infusion pump systems," *Journal of diabetes science and technology*, vol. 9, no. 1, pp. 24–33, 2015.

[19] S. L. Wendt, A. Valeur, H. Madsen, J. B. Jørgensen, and C. B. Knudsen, "Pharmacokinetics modeling of glucagon and a novel glucagon analogue after subcutaneous administration in dogs," in *Diabetes technology & therapeutics*, vol. 17, no. S1, 2015, pp. A-109.

[20] R. Hovorka, F. Shojaee-Moradie, P. V. Carroll, L. J. Chassin, I. J. Gowrie, N. C. Jackson, R. S. Tudor, A. M. Umpleby, and R. H. Jones, "Partitioning glucose distribution/transport, disposal, and endogenous production during IVGTT," *American Journal of Physiology-Endocrinology and Metabolism*, vol. 282, no. 5, pp. E992–E1007, 2002.

[21] A. Haidar, M. E. Wilinska, J. A. Graveston, and R. Hovorka, "Stochastic virtual population of subjects with type 1 diabetes for the assessment of closed-loop glucose controllers," *IEEE Transactions on Biomedical Engineering*, vol. 60, no. 12, pp. 3524–3533, 2013.

[22] J. R. Castle, J. El Youssef, P. A. Bakhtiani, Y. Cai, J. M. Stobbe, D. Branigan, K. Ramsey, P. Jacobs, R. Reddy, M. Woods, and W. K. Ward, "Effect of repeated glucagon doses on hepatic glycogen in type 1 diabetes: Implications for a bihormonal closed-loop system," *Diabetes care*, vol. 38, no. 11, pp. 2115–2119, 2015.

[23] R. Hovorka, V. Canonico, L. J. Chassin, U. Haueter, M. Massi-Benedetti, M. O. Federici, T. R. Pieber, H. C. Schaller, L. Schaupp, T. Vering, and M. E. Wilinska, "Nonlinear model predictive control of glucose concentration in subjects with type 1 diabetes," *Physiological measurement*, vol. 25, no. 4, pp. 905–920, 2004.

[24] C. Dalla Man, F. Micheletto, D. Lv, M. Breton, B. Kovatchev, and C. Cobelli, "The UVA/PADOVA type 1 diabetes simulator: New features," *Journal of diabetes science and technology*, vol. 8, no. 1, pp. 26–34, 2014.

[25] P. Herrero, P. Georgiou, N. Oliver, M. Reddy, D. Johnston, and C. Toumazou, "A composite model of glucagon-glucose dynamics for *in silico* testing of bihormonal glucose controllers," *Journal of diabetes science and technology*, vol. 7, no. 4, pp. 941–951, 2013.

[26] A. Emami, J. El Youssef, R. Rabasa-Lhoret, J. Pineau, J. R. Castle, and A. Haidar, "Modelling glucagon action in patients with type 1 diabetes," 2016, submitted paper.

[27] M. Wada, C. C. Connolly, C. Tarumi, D. W. Neal, and A. D. Cherrington, "Hepatic denervation does not significantly change the response of the liver to glucagon in conscious dogs," *American Journal of Physiology - Endocrinology and Metabolism*, vol. 268, no. 2, pp. E194–E203, 1995.

[28] J. El Youssef, J. R. Castle, P. A. Bakhtiani, A. Haidar, D. L. Branigan, M. Breen, and W. K. Ward, "Quantification of the glycemic response to microdoses of subcutaneous glucagon at varying insulin levels," *Diabetes care*, vol. 37, no. 11, pp. 3054–3060, 2014.

[29] A. Adkins, R. Basu, M. Persson, B. Dicke, P. Shah, A. Vella, W. F. Schwenk, and R. Rizza, "Higher insulin concentrations are required to suppress gluconeogenesis than glycogenolysis in nondiabetic humans," *Diabetes*, vol. 52, no. 9, pp. 2213–2220, 2003.

[30] J. Girard, "The inhibitory effects of insulin on hepatic glucose production are both direct and indirect," *Diabetes*, vol. 55, no. Supplement 2, pp. S65–S69, 2006.

[31] S. Rosenbaum, *Basic pharmacokinetics and pharmacodynamics: An integrated textbook and computer simulations*, 1st ed. John Wiley & Sons, Inc., 2011.

[32] R. N. Bergman, Y. Z. Ider, C. R. Bowden, and C. Cobelli, "Quantitative estimation of insulin sensitivity." *American Journal of Physiology-Endocrinology And Metabolism*, vol. 236, no. 6, pp. E667–E677, 1979.

[33] N. R. Kristensen, H. Madsen, and S. B. Jørgensen, "A method for systematic improvement of stochastic grey-box models," *Computers & chemical engineering*, vol. 28, no. 8, pp. 1431–1449, 2004.

[34] CTSM-R development team. (2015, April) Continuous time stochastic modeling in r: User's guide and reference manual. [Online]. Available: http://ctsm.info/pdfs/ctsmr-reference.pdf

[35] S. L. Wendt, C. B. Knudsen, J. B. Jørgensen, H. Madsen, and A. Haidar, "Modelling the glucose-insulin-glucagon dynamics after subcutaneous administration of native glucagon and a novel glucagon analogue in dogs," in *Diabetes technology & therapeutics*, vol. 18, no. S1, 2016, pp. A-134.

[36] Roche custom biotech. (2011) Glucose test principle. [Online]. Available: http://custombiotech.roche.com/content/dam/internet/dia/custombiotech/custombiotech_com/en_GB/pdf/Glucose_Test_Principle_05837804990_03.11.pdf

[37] D. C. Simonson and R. A. DeFronzo, "Glucagon physiology and aging: evidence for enhanced hepatic sensitivity," *Diabetologia*, vol. 25, no. 1, pp. 1–7, 1983.

[38] D. Matthews, J. Hosker, A. Rudenski, B. Naylor, D. Treacher, and R. Turner, "Homeostasis model assessment: insulin resistance and β-cell function from fasting plasma glucose and insulin concentrations in man," *Diabetologia*, vol. 28, no. 7, pp. 412–419, 1985.

[39] A. Haidar, D. Elleri, K. Kumareswaran, L. Leelarathna, J. M. Allen, K. Caldwell, H. R. Murphy, M. E. Wilinska, C. L. Acerini, M. L. Evans, D. B. Dunger, M. Nodale, and R. Hovorka, "Pharmacokinetics of insulin aspart in pump-treated subjects with type 1 diabetes: reproducibility and effect of age, weight, and duration of diabetes," *Diabetes Care*, vol. 36, no. 10, pp. e173–e174, 2013.

[40] A. Haidar, C. Duval, L. Legault, and R. Rabasa-Lhoret, "Pharmacokinetics of insulin aspart and glucagon in type 1 diabetes during closed-loop operation," *Journal of diabetes science and technology*, vol. 7, no. 6, pp. 1507–1512, 2013.

[41] A. D. Cherrington, J. E. Liljenquist, G. I. Shulman, P. E. Williams, and W. W. Lacy, "Importance of hypoglycemia-induced glucose production during isolated glucagon deficiency." *American Journal of Physiology - Endocrinology and Metabolism*, vol. 236, no. 3, pp. E263–E271, 1979.

[42] M. A. Davis, P. E. Williams, and A. D. Cherrington, "Effect of glucagon on hepatic lactate metabolism in the conscious dog," *American Journal of Physiology - Endocrinology and Metabolism*, vol. 248, no. 4, pp. E463–E470, 1985.

[43] M. A. Felmlee, M. E. Morris, and D. E. Mager, "Mechanism-based pharmacodynamic modeling," *Methods in Molecular Biology*, vol. 929, pp. 583–600, 2012.

[44] C. Kreutz, A. Raue, D. Kaschek, and J. Timmer, "Profile likelihood in systems biology," *The FEBS Journal*, vol. 208, pp. 2564–2571, 2013.

[45] H. Madsen and P. Thyregod, *Introduction to general and generalized linear models*. CRC Press, 2011.

[46] N. R. Kristensen, H. Madsen, and S. B. Jørgensen, "Parameter estimation in stochastic grey-box models," *Automatica*, vol. 40, no. 2, pp. 225–237, 2004.

[47] R. Juhl, J. K. Møller, J. B. Jørgensen, and H. Madsen, *Prediction Methods for Blood Glucose Concentration*. Springer, 2016, ch. Modeling and prediction using stochastic differential equations.

[48] J. K. Møller, J. Carstensen, and H. Madsen, "Structural identification and validation in stochastic differential equation based models - with application to a marine ecosystem NP-model," *Journal of the Royal Statistical Society, Series C*, 2011.

[49] H. Madsen, *Time series analysis*. CRC Press, 2007.

[50] H. Blauw, I. Wendl, J. H. DeVries, T. Heise, and T. Jax, "Pharmacokinetics and pharmacodynamics of various glucagon dosages at different blood glucose levels," *Diabetes, Obesity and Metabolism*, vol. 18, no. 1, pp. 34–39, 2016.

[51] A. Ranjan, S. Schmidt, S. Madsbad, J. J. Holst, and K. Nørgaard, "Effects of subcutaneous, low-dose glucagon on insulin-induced mild hypoglycaemia in patients with insulin pump treated type 1 diabetes." *Diabetes, obesity & metabolism*, vol. Epub ahead of print, 2016.

[52] C. J. Graf, J. R. Woodworth, M. E. Seger, J. H. Holcombe, R. R. Bowsher, and R. Lynch, "Pharmacokinetic and glucodynamic comparisons of recombinant and animal-source glucagon after IV, IM, and SC injection in healthy volunteers," *Journal of pharmaceutical sciences*, vol. 88, no. 10, pp. 991–995, 1999.

Appendix

A Raw data

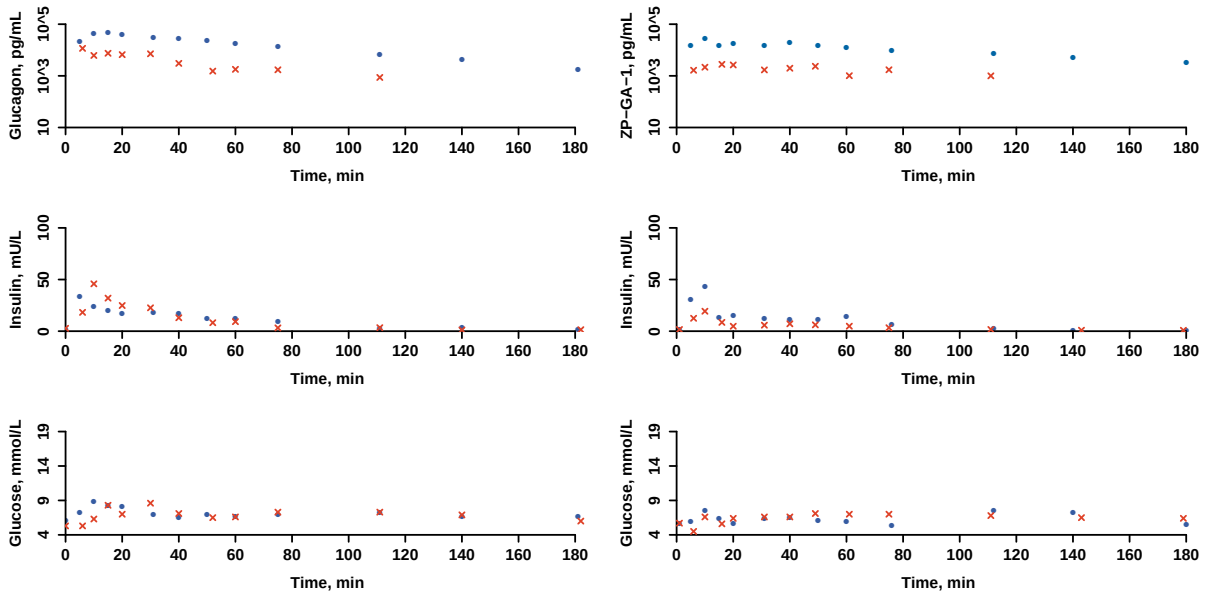

Figure 16: Raw PK and PD data with outliers measured in dog 1. Data from low or high doses of glucagon and ZP-GA-1 are red crosses or blue dots, respectively.

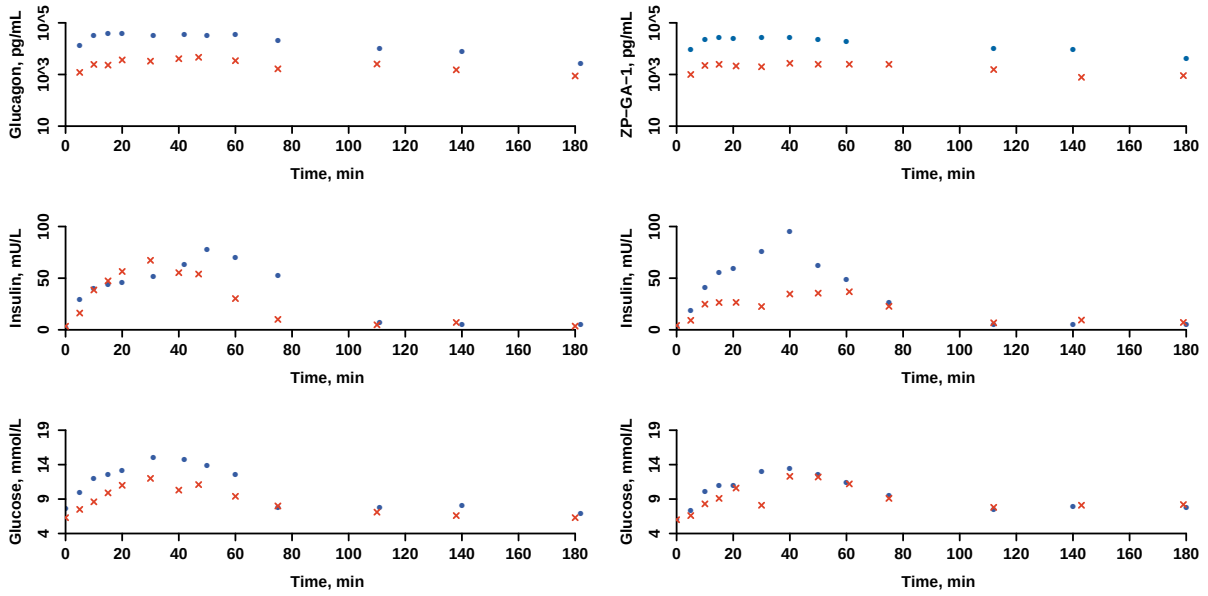

Figure 17: Raw PK and PD data with outliers measured in dog 2. Data from low or high doses of glucagon and ZP-GA-1 are red crosses or blue dots, respectively.

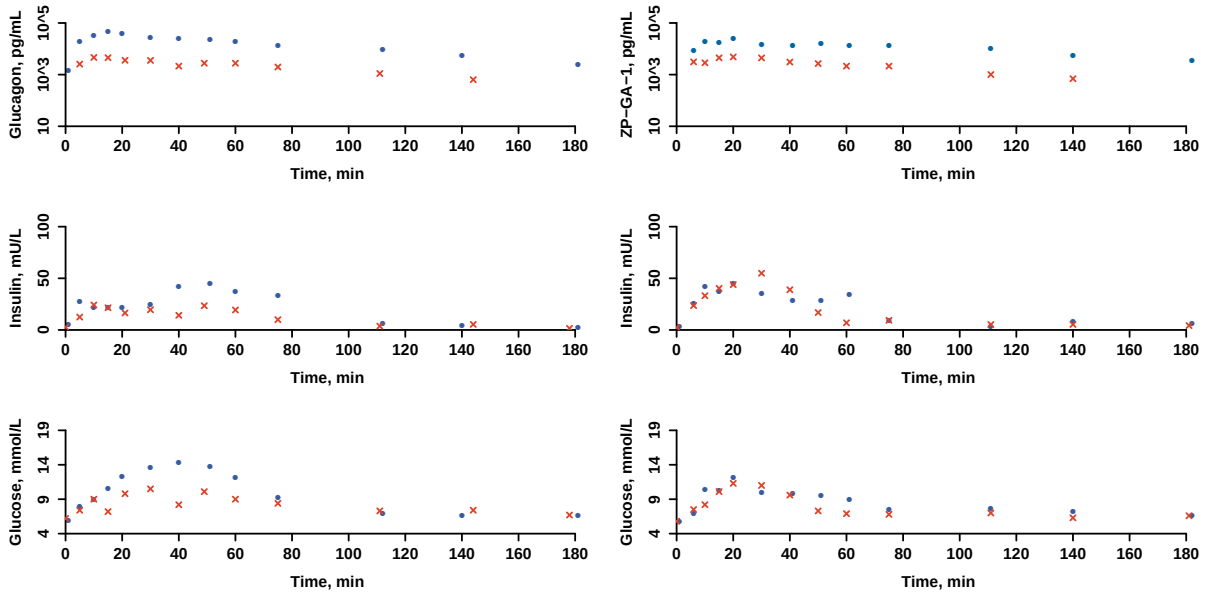

Figure 18: Raw PK and PD data with outliers measured in dog 3. Data from low or high doses of glucagon and ZP-GA-1 are red crosses or blue dots, respectively.

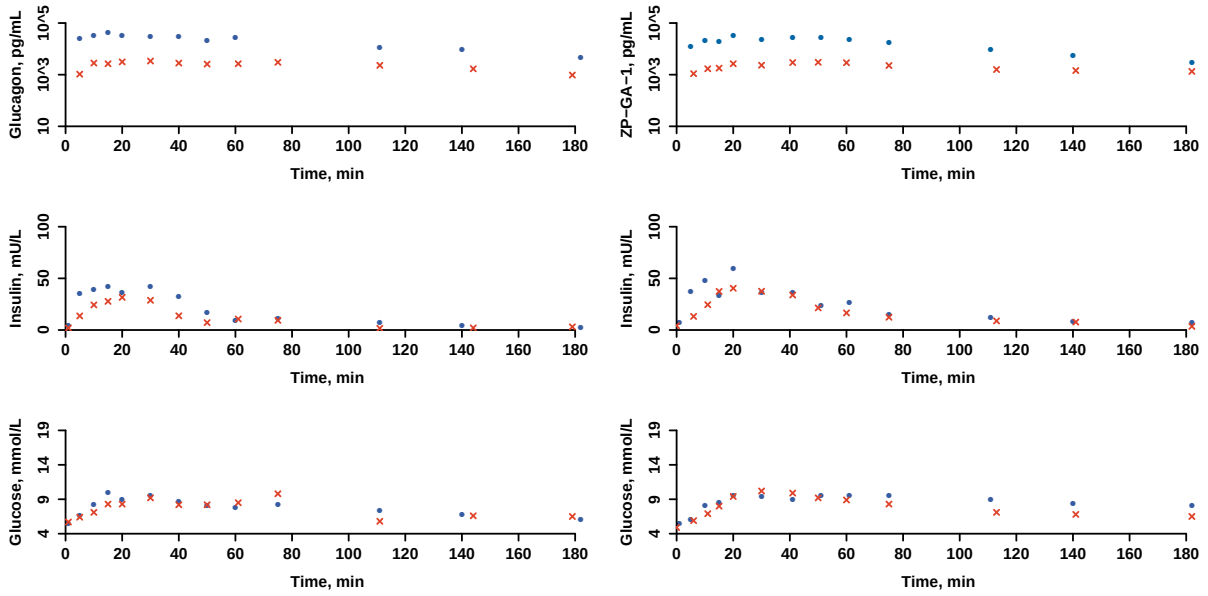

Figure 19: Raw PK and PD data with outliers measured in dog 4. Data from low or high doses of glucagon and ZP-GA-1 are red crosses or blue dots, respectively.

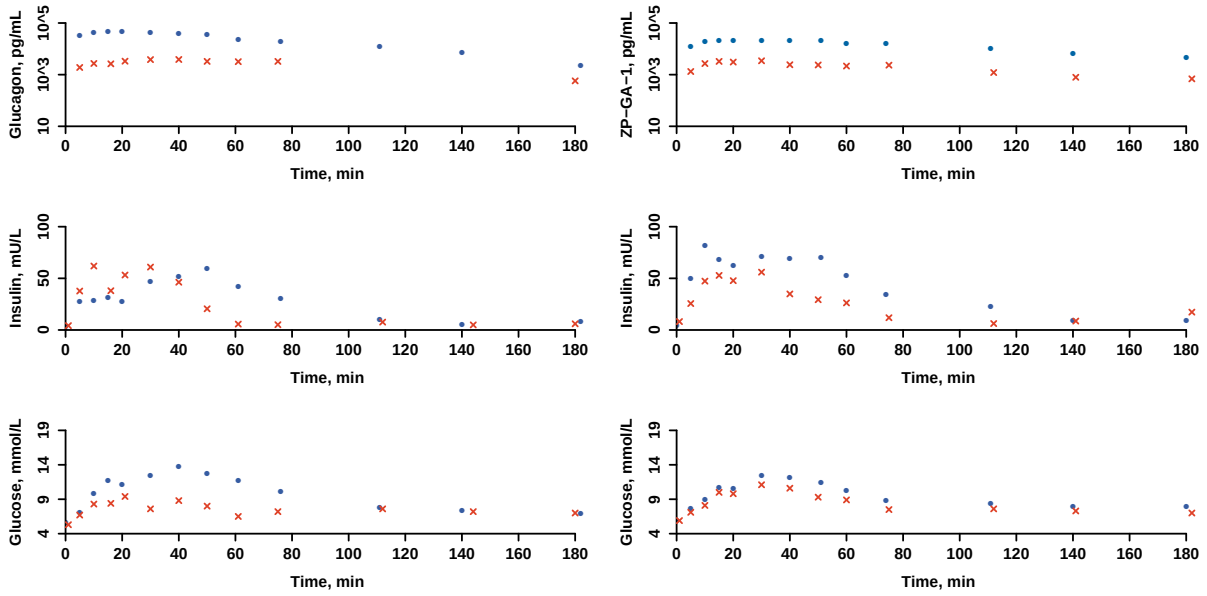

Figure 20: Raw PK and PD data with outliers measured in dog 5. Data from low or high doses of glucagon and ZP-GA-1 are red crosses or blue dots, respectively.

B PK Model fits

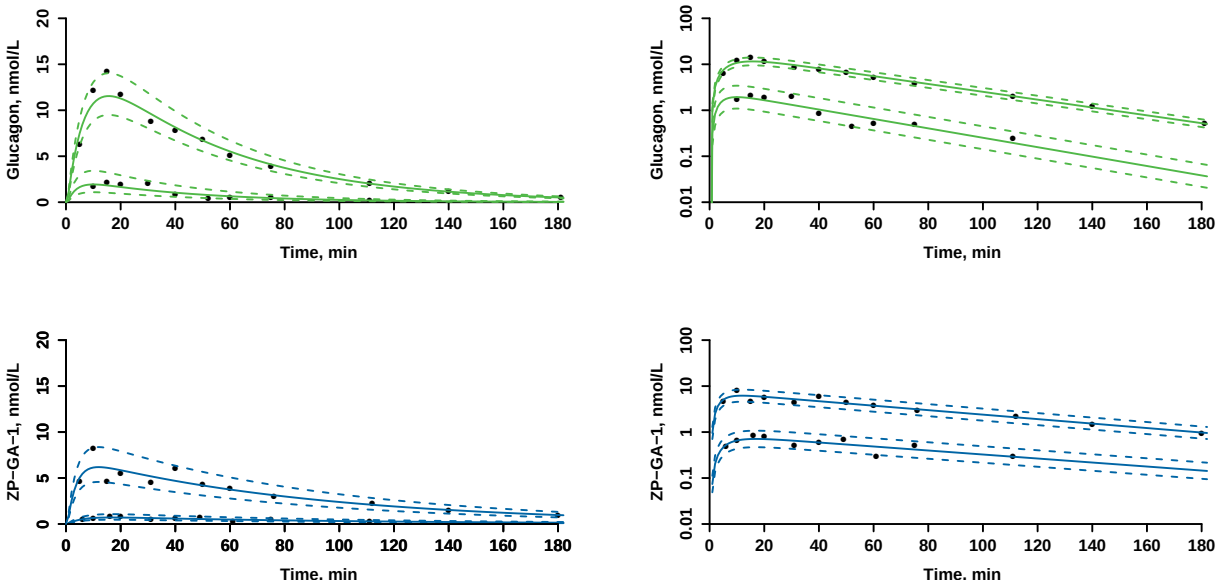

Figure 21: PK model fit after low and high doses of glucagon (green) and ZP-GA-1 (blue) in dog 1. Left graphs are with regular axes and right graphs are with $\log_{10}$ axes.

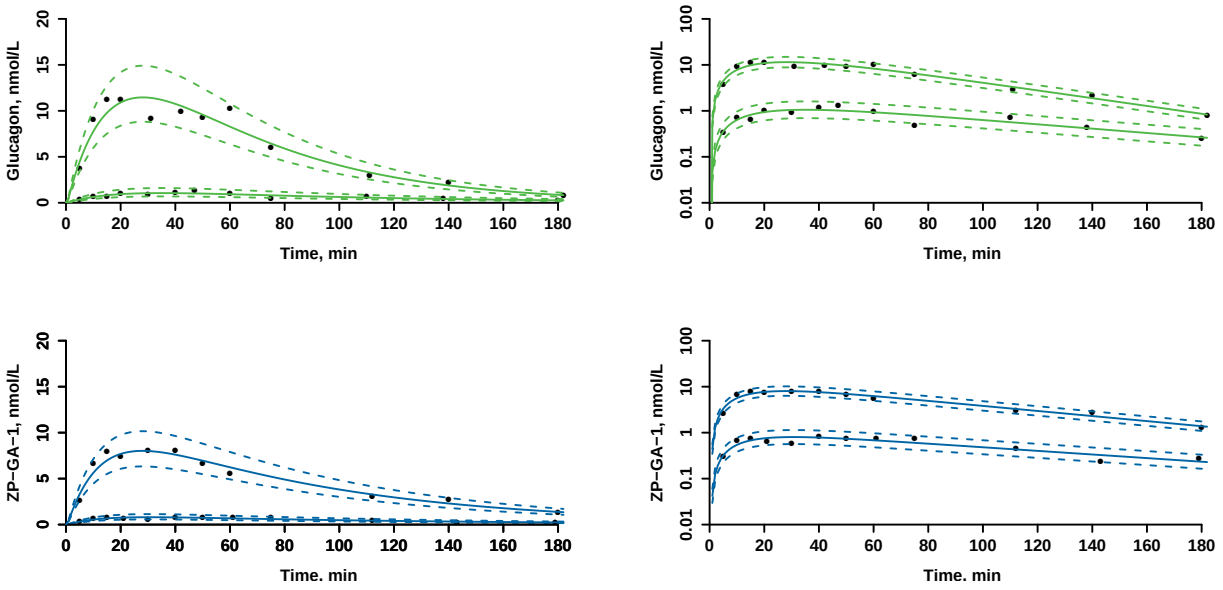

Figure 22: PK model fit after low and high doses of glucagon (green) and ZP-GA-1 (blue) in dog 2. Left graphs are with regular axes and right graphs are with $\log_{10}$ axes.

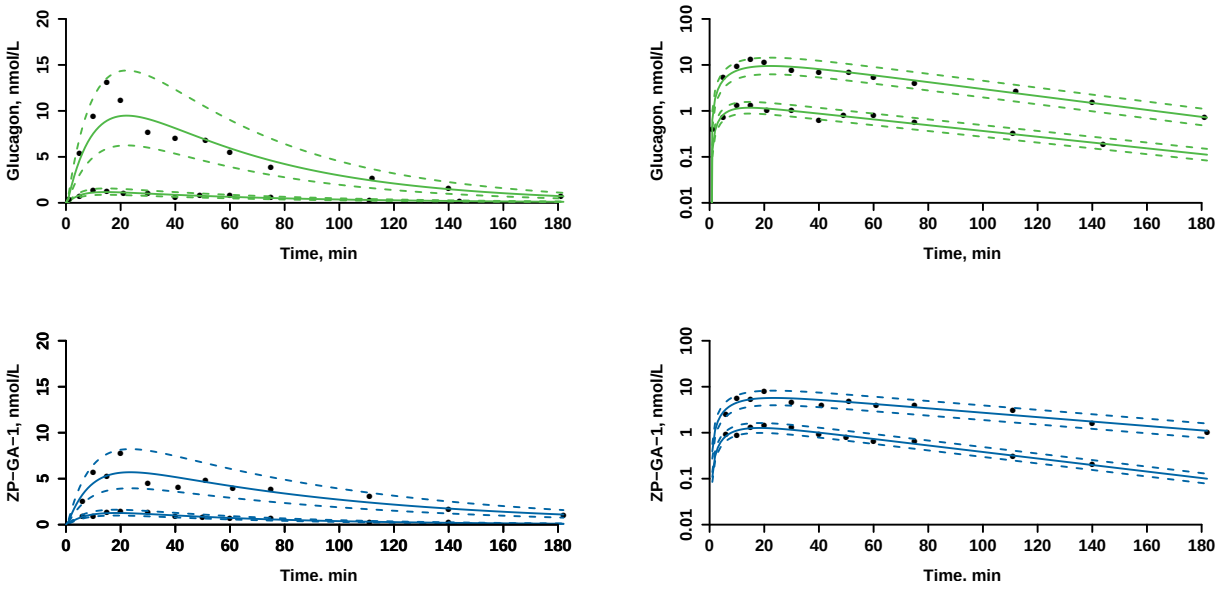

Figure 23: PK model fit after low and high doses of glucagon (green) and ZP-GA-1 (blue) in dog 3. Left graphs are with regular axes and right graphs are with $\log_{10}$ axes.

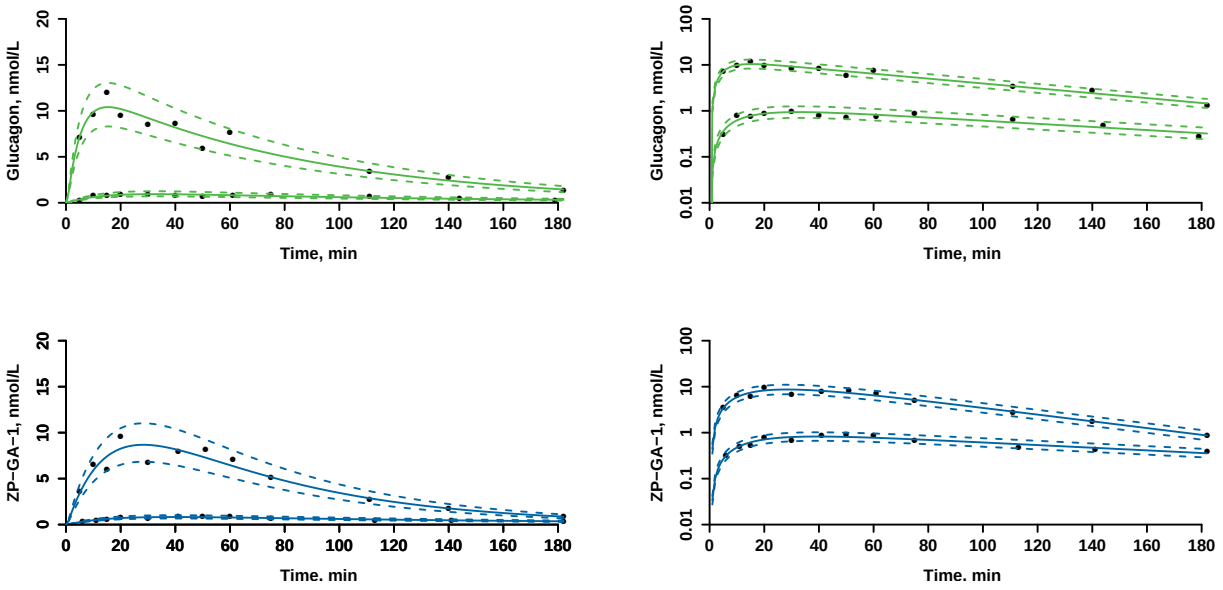

Figure 24: PK model fit after low and high doses of glucagon (green) and ZP-GA-1 (blue) in dog 4. Left graphs are with regular axes and right graphs are with $\log_{10}$ axes.

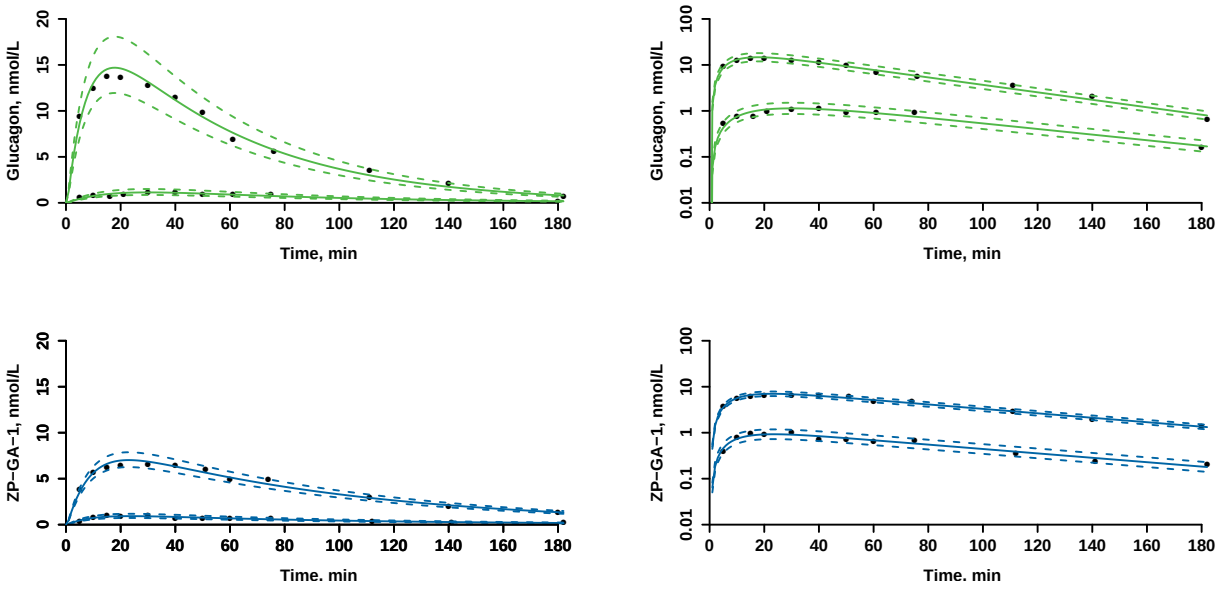

Figure 25: PK model fit after low and high doses of glucagon (green) and ZP-GA-1 (blue) in dog 5. Left graphs are with regular axes and right graphs are with $\log_{10}$ axes.

C PD model fits

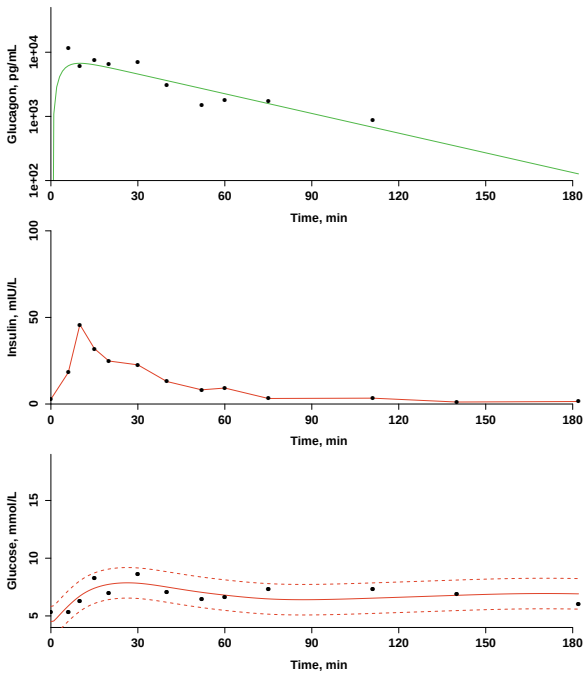

(a) 20 nmol/kg of glucagon.

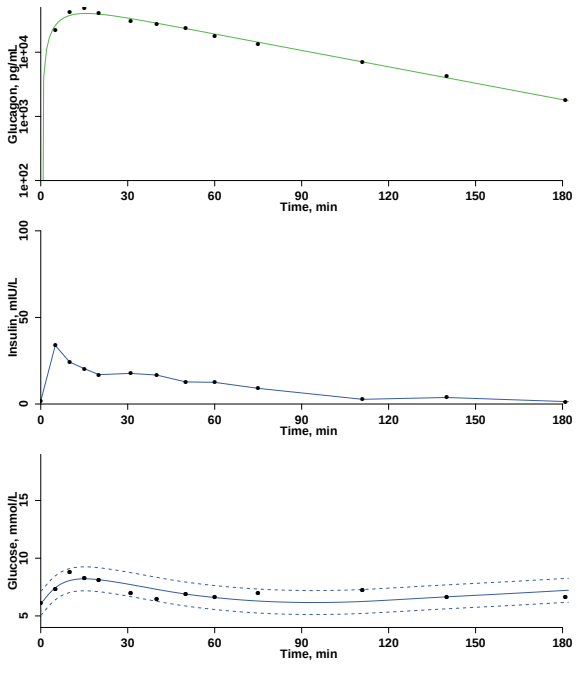

(b) 120 nmol/kg of glucagon.

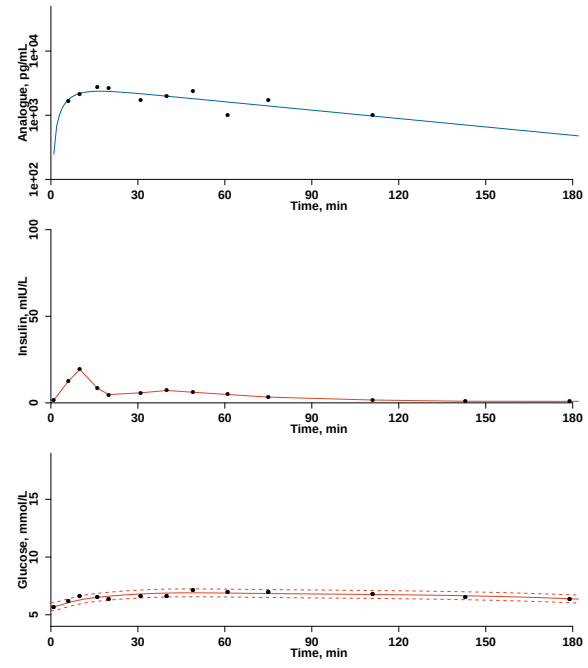

(c) 20 nmol/kg of ZP-GA-1.

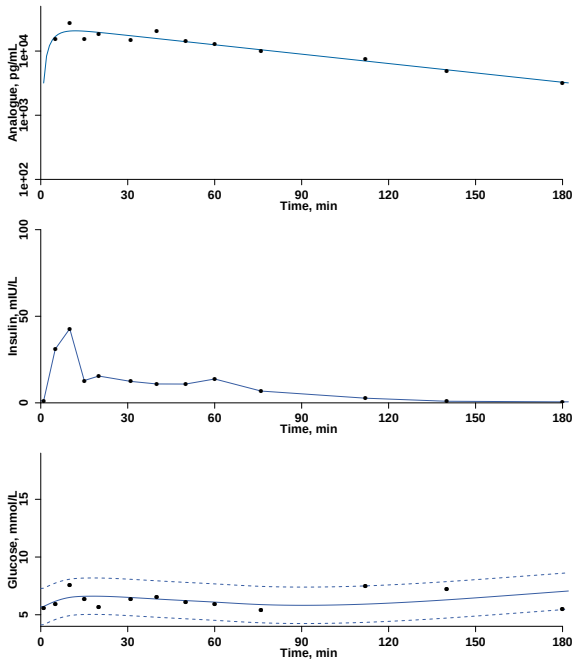

(d) 120 nmol/kg of ZP-GA-1.

Figure 26: Plasma concentrations of PD model inputs glucagon and insulin together with PD model fit of glucose in dog 1. Administered doses and drugs are written in each subfigure.

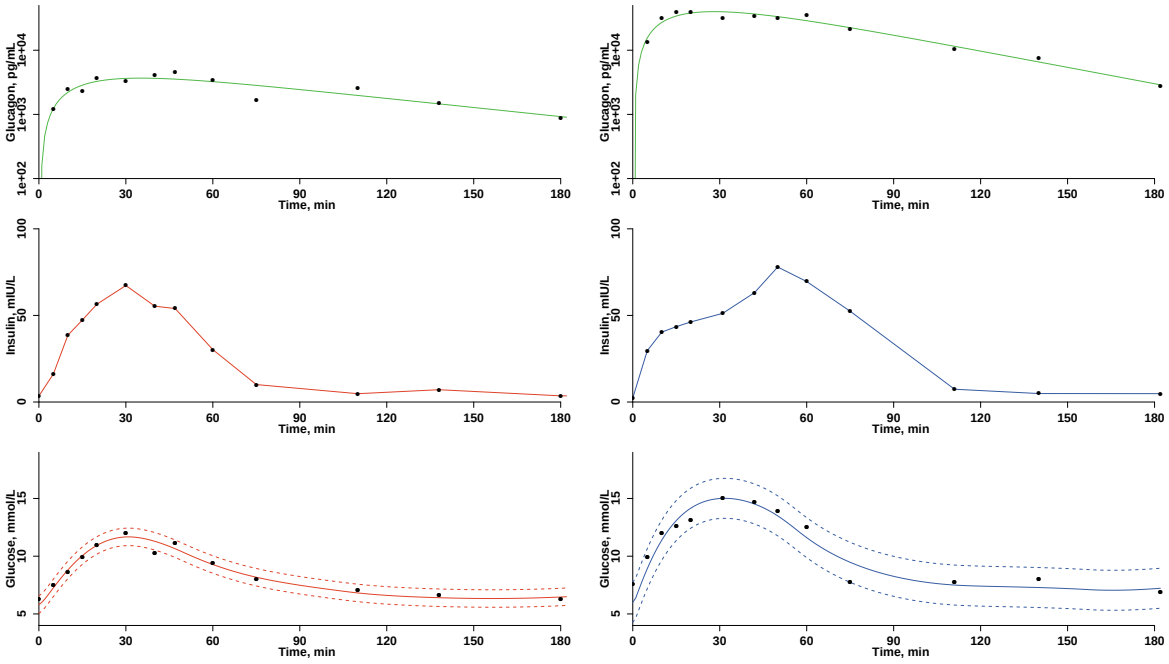

(a) 20 nmol/kg of glucagon.

(b) 120 nmol/kg of glucagon.

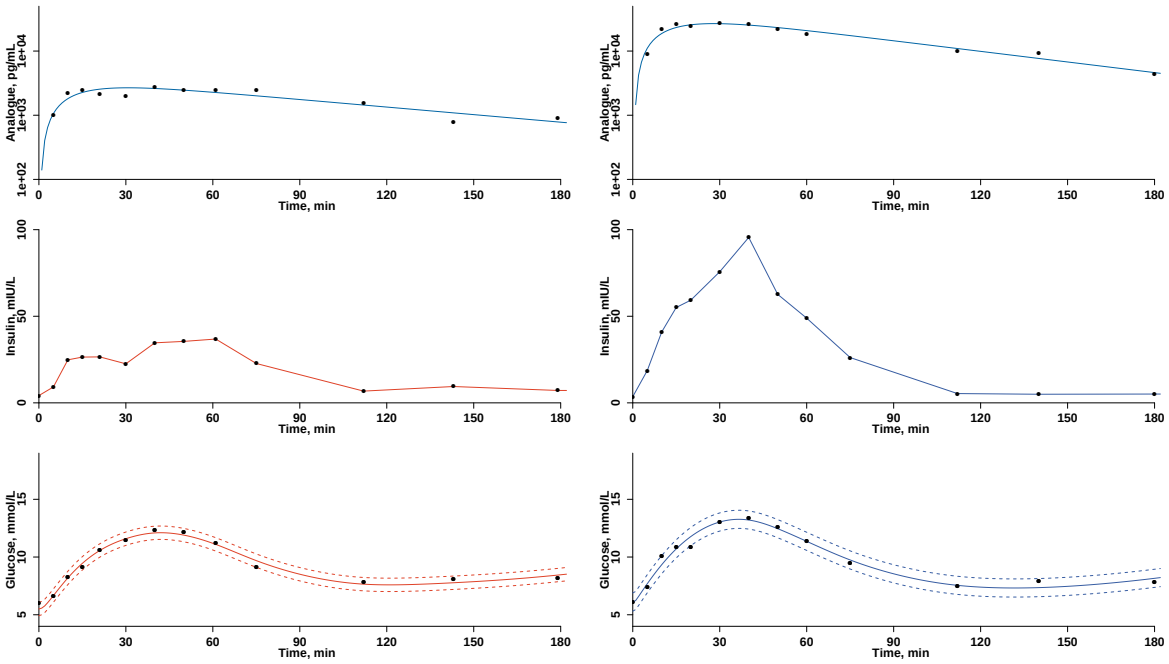

(c) 20 nmol/kg of ZP-GA-1.

(d) 120 nmol/kg of ZP-GA-1.

Figure 27: Plasma concentrations of PD model inputs glucagon and insulin together with PD model fit of glucose in dog 2. Administered doses and drugs are written in each subfigure.

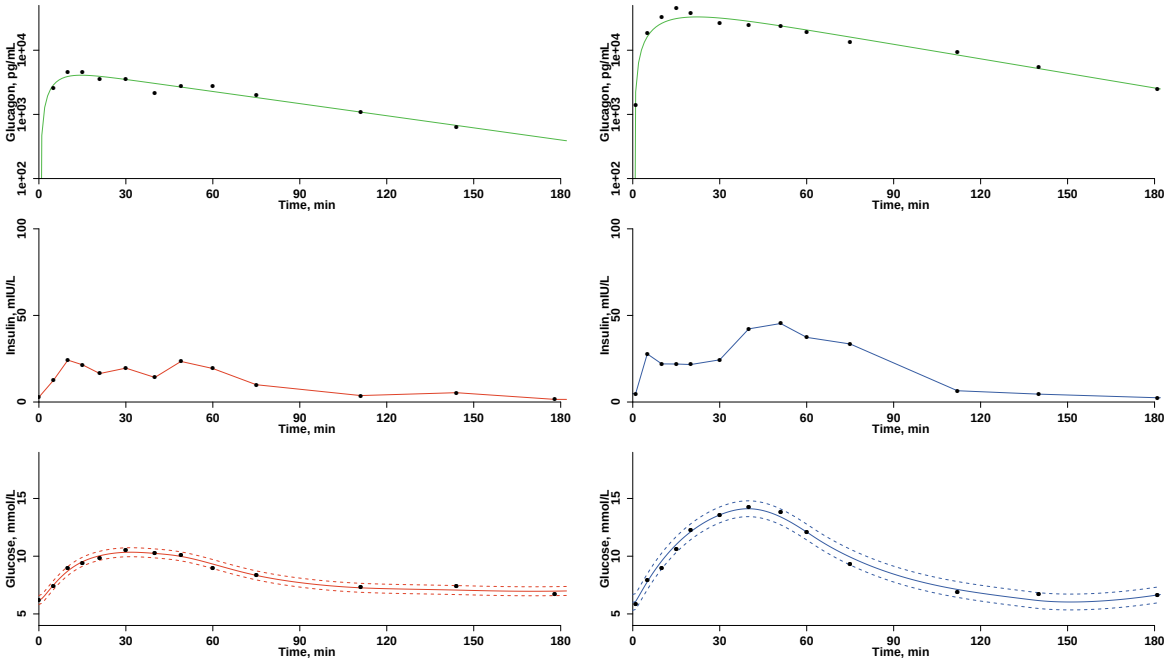

(a) 20 nmol/kg of glucagon.

(b) 120 nmol/kg of glucagon.

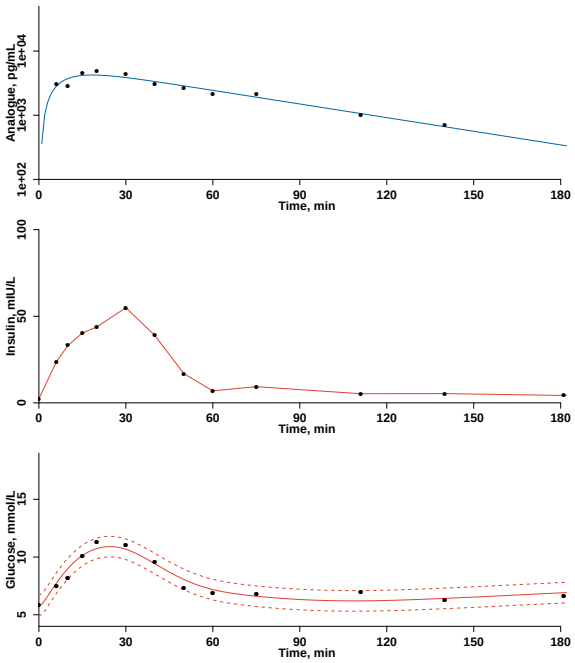

(c) 20 nmol/kg of ZP-GA-1.

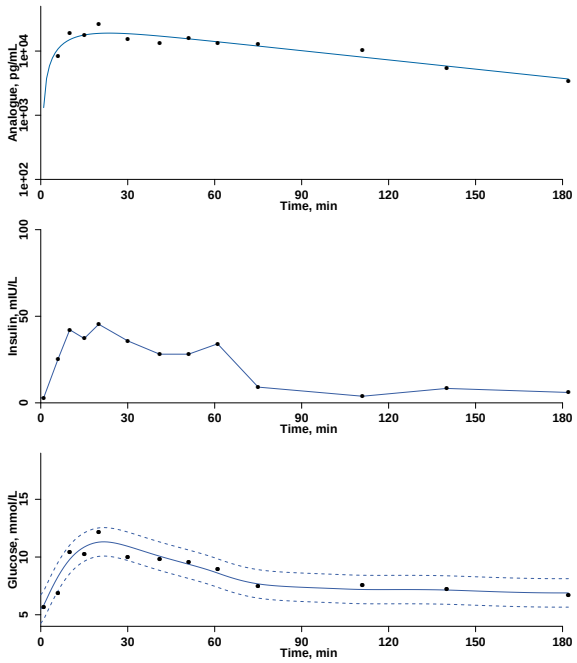

(d) 120 nmol/kg of ZP-GA-1.

Figure 28: Plasma concentrations of PD model inputs glucagon and insulin together with PD model fit of glucose in dog 3. Administered doses and drugs are written in each subfigure.

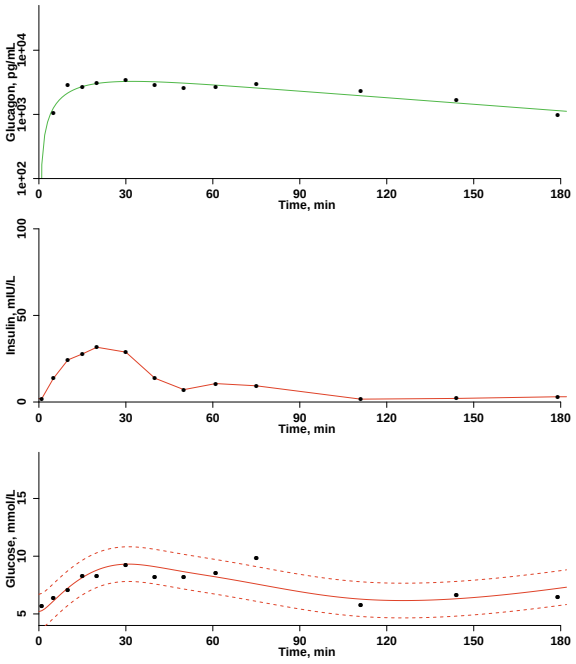

(a) 20 nmol/kg of glucagon.

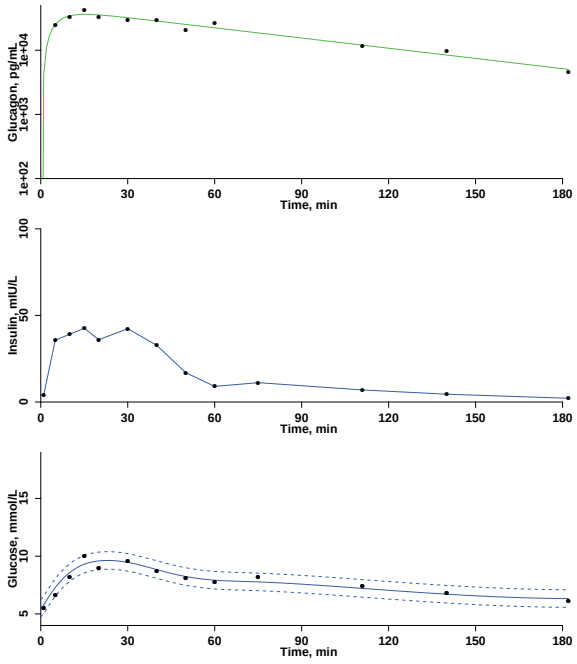

(b) 120 nmol/kg of glucagon.

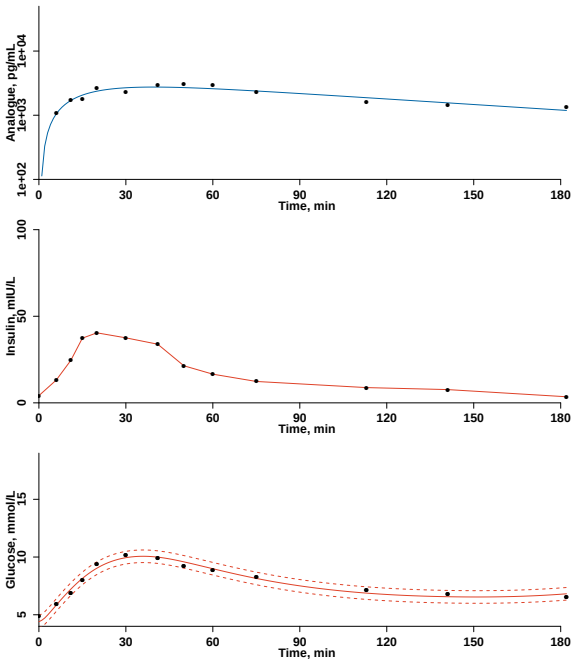

(c) 20 nmol/kg of ZP-GA-1.

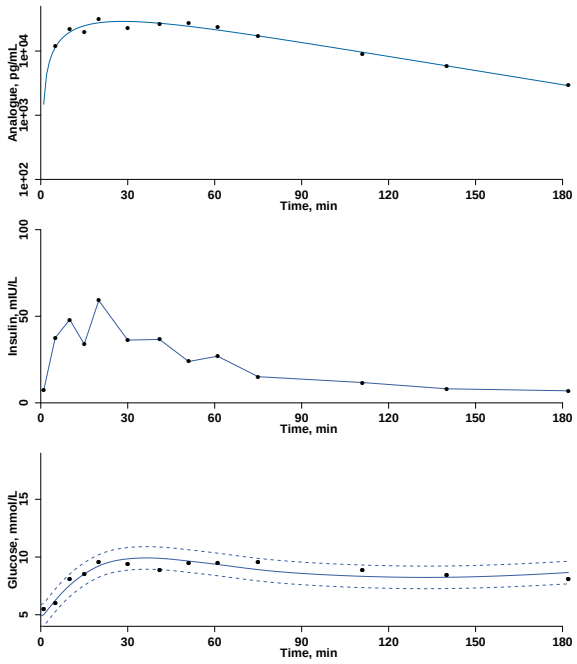

(d) 120 nmol/kg of ZP-GA-1.

Figure 29: Plasma concentrations of PD model inputs glucagon and insulin together with PD model fit of glucose in dog 4. Administered doses and drugs are written in each subfigure.

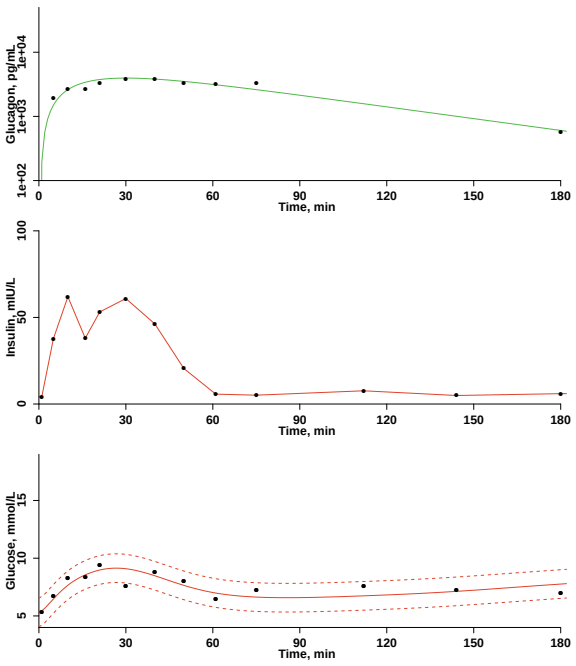

(a) 20 nmol/kg of glucagon.

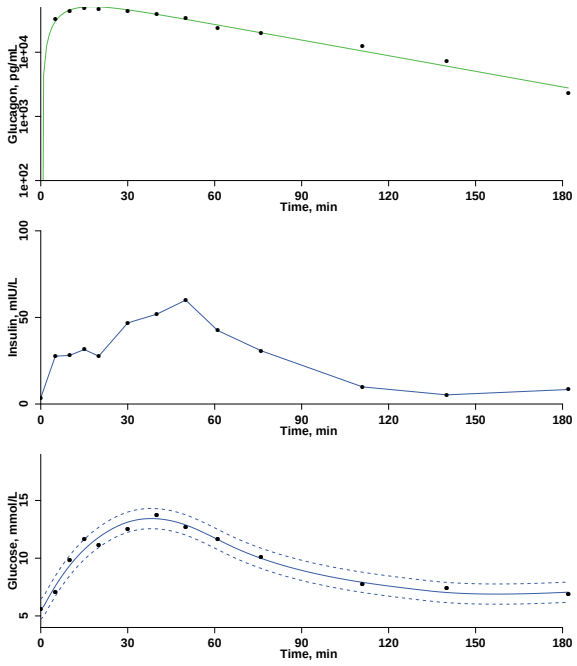

(b) 120 nmol/kg of glucagon.

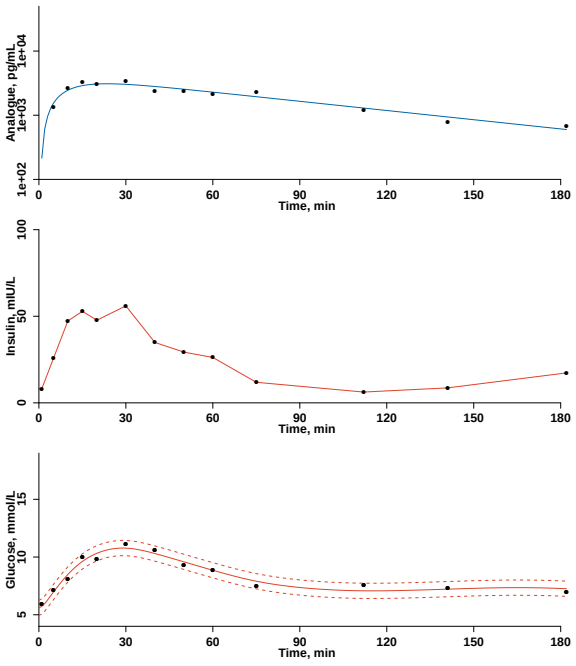

(c) 20 nmol/kg of ZP-GA-1.

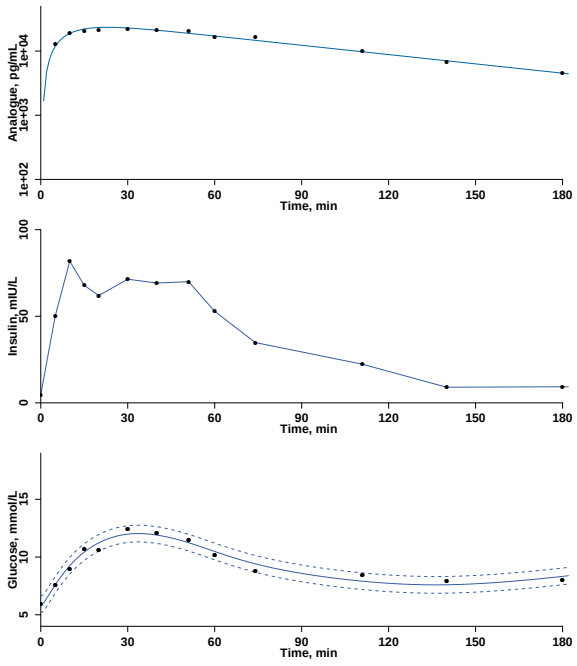

(d) 120 nmol/kg of ZP-GA-1.

Figure 30: Plasma concentrations of PD model inputs glucagon and insulin together with PD model fit of glucose in dog 5. Administered doses and drugs are written in each subfigure.